Ontogeny of human mucosal-associated invariant T cells and related T cell subsets.

Ghada Ben Youssef, Marie Tourret, Marion Salou, Liana Ghazarian, Véronique Houdouin, Stanislas Mondot, Yvonne Mburu, Marion Lambert, Saba Azarnoush, Jean-Sebastien Diana, et al.

Published Online: 16 January, 2018 | Supp Info: http://doi.org/10.1084/jem.20171739

JEM

Article

Ontogeny of human mucosal-associated invariant T cells and related T cell subsets

Ghada Ben Youssef,[1]* Marie Tourret,[1]* Marion Salou,[2]* Liana Ghazarian,[1]* Véronique Houdouin,[1,3] Stanislas Mondot,[2] Yvonne Mburu,[2] Marion Lambert,[1] Saba Azarnoush,[1] Jean-Sébastien Diana,[1] Anne-Laure Virlouvet,[4] Michel Peuchmaur,[1,5] Thomas Schmitz,[6] Jean-Hugues Dalle,[1,7]** Olivier Lantz,[2,8,9,10]** Valérie Biran,[4]** and Sophie Caillat-Zucman[1,11]

[1]Institut national de recherche médicale (INSERM) UMR1149, Center for Research on Inflammation, Paris Diderot University, Paris, France
[2]Institut Curie, PSL Research University, INSERM U932, Paris, France
[3]Service de Gastroentérologie et Pneumologie Pédiatrique, [4]Service de Pédiatrie et Réanimation Néonatale, [5]Service de Pathologie Pédiatrique, [6]Service d'Obstétrique, and [7]Service d'Hématologie Pédiatrique, Hôpital Robert Debré, Assistance Publique-Hôpitaux de Paris, Paris, France
[8]Centre d'Investigations Cliniques CIC-BT1428 IGR/Curie, Paris, France
[9]Equipe labellisée de la Ligue de Lutte contre le Cancer and [10]Département de Biopathologie, Institut Curie, Paris, France
[11]Laboratoire d'Immunologie, Hôpital Saint-Louis, Assistance Publique-Hôpitaux de Paris, Paris, France

Mucosal-associated invariant T (MAIT) cells are semi-invariant Vα7.2$^+$ CD161^{high}CD4$^-$ T cells that recognize microbial riboflavin precursor derivatives such as 5-OP-RU presented by MR1. Human MAIT cells are abundant in adult blood, but there are very few in cord blood. We longitudinally studied Vα7.2$^+$ CD161^{high} T cell and related subset levels in infancy and after cord blood transplantation. We show that Vα7.2$^+$ and Vα7.2$^-$ CD161^{high} T cells are generated early during gestation and likely share a common prenatal developmental program. Among cord blood Vα7.2$^+$ CD161^{high} T cells, the minority recognizing MR1:5-OP-RU display a TRAV/TRBV repertoire very similar to adult MAIT cells. Within a few weeks of life, only the MR1:5-OP-RU reactive Vα7.2$^+$ CD161^{high} T cells acquire a memory phenotype. Only these cells expand to form the adult MAIT pool, diluting out other Vα7.2$^+$ CD161^{high} and Vα7.2$^-$ CD161^{high} populations, in a process requiring at least 6 years to reach adult levels. Thus, the high clonal size of adult MAIT cells is antigen-driven and likely due to the fine specificity of the TCRαβ chains recognizing MR1-restricted microbial antigens.

INTRODUCTION

Mucosal-associated invariant T (MAIT) cells are nonconventional CD3$^+$ CD4$^-$ CD161^{high} T lymphocytes, which express a semi-invariant TCR (Vα7.2-Jα33/20/12 in humans, Vα19-Jα33 in mice, combined with a restricted set of Vβ chains; Tilloy et al., 1999; Treiner et al., 2003; Reantragoon et al., 2013; Lepore et al., 2014). MAIT TCRs recognize microbial-derived riboflavin (vitamin B2) biosynthesis intermediate derivatives, such as 5-(2-oxopropylideneamino)-6-D-ribitylaminouracil (5-OP-RU), presented by the monomorphic MHC class I-related molecule (MR1; Treiner et al., 2003; Kjer-Nielsen et al., 2012; Corbett et al., 2014). MAIT cells are preferentially localized in mucosal tissues, including gut and lung, and the liver and represent the most abundant innate-like T cell population in human peripheral blood, comprising up to 10% of the entire T cell population (Martin et al., 2009; Dusseaux et al., 2011). This compares with just 0.1% for natural killer T (NKT) cells, another population of semi-invariant innate-like T cells recognizing glycolipids presented by CD1d. Upon recognition of microbial antigens, MAIT cells display immediate effector responses by secreting inflammatory cytokines and mediating cytotoxicity against bacterially infected cells (Gold et al., 2010; Dusseaux et al., 2011; Le Bourhis et al., 2013; Kurioka et al., 2015; Dias et al., 2017). Thus, MAIT cells have emerged as potentially crucial for antimicrobial defense (Le Bourhis et al., 2010; Georgel et al., 2011; Meierovics et al., 2013; Leung et al., 2014; Smith et al., 2014; Booth et al., 2015; Meierovics and Cowley, 2016; Chen et al., 2017). In addition to microbial products derived from vitamin B2 synthesis, other MR1-binding ligands have been identified, including the nonstimulatory folic acid derivative 6-formyl-pterin (6-FP; Kjer-Nielsen et al., 2012), and various activating and nonactivating drugs and drug-like molecules (Keller et al., 2017b), but the clinical relevance of these ligands is yet to be elucidated. Finally, MAIT cells can respond to a combination of cytokines, such as IL-12 and IL-18, in an MR1-independent fashion (Ussher et al., 2014; Slichter et al., 2016), further extending their potential participation in

*G. Ben Youssef, M. Tourret, M. Salou, and L. Ghazarian contributed equally to this paper.

**J.-H. Dalle, O. Lantz, and V. Biran contributed equally to this paper.

Correspondence to Sophie Caillat-Zucman: sophie.caillat@inserm.fr

The Rockefeller University Press
J. Exp. Med. 2018 Vol. 215 No. 2 459–479
https://doi.org/10.1084/jem.20171739

Journal of Experimental Medicine

a wide array of inflammatory conditions (Loh et al., 2016; van Wilgenburg et al., 2016).

At birth, adaptive immunity is naive in the absence of in utero exposure to antigens. Maturation of the immune response occurs gradually after birth in response to antigenic stimulation from the environment (Adkins et al., 2004; Levy, 2007). In the absence of a fully developed adaptive immunity, newborns are heavily dependent on innate immunity for the control and prevention of infections during the first months of life (Kollmann et al., 2017). Preterm neonates suffer a high frequency and severity of microbial infections, many of them occurring spontaneously across epithelial barriers because of the immaturity of the immune system. Because MAIT cells represent a large pool of T cells able to rapidly respond to a wide range of microorganisms, they might be crucial for newborn immunity before the maturation of the specific and long-term memory adaptive immunity.

How and when human MAIT cells develop and differentiate after birth remains, however, little explored. MAIT cells represent only a very small fraction of cord blood T cells but, in contrast, are predominant in adult blood (Martin et al., 2009; Dusseaux et al., 2011; Walker et al., 2012), indicating that thymopoiesis is complemented by an important postnatal peripheral expansion. Using MR1:5-OP-RU tetramers, Koay et al. (2016) recently delineated a three-stage developmental pathway for mouse and human MAIT populations. Immature stage 1 and stage 2 MAIT cells (tetramer^{pos} Vα7.2$^+$ CD161$^-$ in humans) predominate in the thymus but represent minor subsets in periphery, where mature stage 3 MAIT cells (tetramer^{pos} Vα7.2$^+$ CD161^{high}) are largely predominant. In mice, MAIT cell maturation requires the promyelocytic leukemia zinc finger (PLZF) transcription factor and commensal microbiota (Martin et al., 2009; Koay et al., 2016). However, studies in mice are not really contributive to understand the mechanisms driving postnatal MAIT development in the human, because of fundamental differences regarding the maturity of the immune system at birth and the frequency of MAIT cells (Cui et al., 2015; Rahimpour et al., 2015). Owing to the difficulty of performing longitudinal studies in infants, only a couple cross-sectional studies have been conducted on small cohorts, showing that MAIT frequency gradually increased with age in the peripheral blood (Dusseaux et al., 2011; Koay et al., 2016). However, comprehensive analysis across the ages is lacking. In addition, it can be discussed whether MAIT cells are defined as Vα7.2$^+$ CD161^{high} cells selected by the restricting MR1 molecule expressed by CD4$^+$CD8$^+$ thymocytes leading to PLZF expression or only as T cells binding to the MR1:5-OP-RU tetramer (Keller et al., 2017a; Legoux et al., 2017).

Here, we analyzed the postnatal expansion and maturation of Vα7.2$^+$ CD161^{high} CD4$^-$ T cells in large series of newborns, according to gestational age and environmental factors. We also studied their recovery in children after unrelated cord blood transplantation, another clinical situation that heavily depends on innate immunity for the control and prevention of infections. In both clinical settings, we show that the extrathymic development of Vα7.2$^+$ CD161^{high} T cells follows a stepwise program, with an early maturation step contrasting with a very slowly progressive expansion. This postnatal developmental scheme is not observed in the Vα7.2$^+$ CD161^{high} MR1:5-OP-RU tetramer^{neg} and Vα7.2$^-$ CD161^{high} populations, which are both much more abundant in the cord blood than Vα7.2$^+$ CD161^{high} MR1:5-OP-RU tetramer^{pos} T cells. Strikingly, MR1:5-OP-RU tetramer^{pos} cells very rapidly predominate among Vα7.2$^+$ CD161^{high} T cells after birth, becoming the vast majority by 6 mo of age. Molecular analysis of the TCR repertoire suggests that only a few clones found in cord blood naive Vα7.2$^+$ CD161^{high} T cells expand after birth to reach high clonal size in adult blood, probably because of their unique ability to recognize MR1-restricted microbial antigens.

RESULTS

Vα7.2$^+$ CD161^{high} T cell frequency in the blood at birth is low and inversely correlated with gestational age

In humans, until MR1:5-OP-RU tetramers were available, MAIT cells were identified as T cells expressing the Vα7.2 TCRα segment and high level of CD161 among CD3$^+$ $\gamma\delta^-$ CD4$^-$ cells. In adult blood, this population fully overlaps with the population labeled by MR1:5-OP-RU tetramers (Reantragoon et al., 2013). In cord blood however, the frequency of tetramer^{pos} Vα7.2$^+$ CD161^{high} T cells is much lower than in adult blood (Koay et al., 2016), but the exact correspondence between Vα7.2$^+$ CD161^{high} cells and MR1:5-OP-RU tetramer^{pos} cells remains unclear. As MR1 tetramers were not available when starting the present study, we analyzed the presence of the Vα7.2-Jα33 rearrangement (TRAV1-2 TRAJ33) by quantitative PCR (qPCR) in sorted Vα7.2$^+$ CD161^{high} and Vα7.2$^+$ CD161$^-$ populations from cord blood and adult blood CD4$^-$ T cells (Fig. 1 A). The Vα7.2-Jα33 rearrangement was 3.4 times less represented in the Vα7.2$^+$ CD161^{high} fraction from cord blood compared with adult blood. Of note, this rearrangement was still overrepresented (3.6 times) in the cord blood Vα7.2$^+$ CD161^{high} subset compared with the CD161$^-$ one. Thus, as in adult blood, the Vα7.2$^+$ CD161^{high} population from cord blood, but not the CD161$^-$ one, encompasses T cells bearing the Vα7.2-Jα33 rearrangement characteristic of MAIT cells.

These results were confirmed and extended by using deep sequencing of the TRAV1-2 gene and quantification of the canonical MAIT TCR (TRAV1-2 TRAJ33/20/12 and 12–amino acid–long CDR3) in sorted Vα7.2$^+$ CD161^{high} and Vα7.2$^+$ CD161$^-$ populations from cord blood and adult blood (Fig. 1 B, left). Although canonical MAIT TCRs were 5.7 times less frequent in the Vα7.2$^+$ CD161^{high} fraction from cord blood compared with adult blood (mean ±16.6% and 95.7%, respectively), they were still identified at a much higher frequency than in the Vα7.2$^+$ CD161$^-$ population, both in cord blood and adult blood. Moreover, we found that the cord blood Vα7.2$^+$ CD161^{high} population was not en-

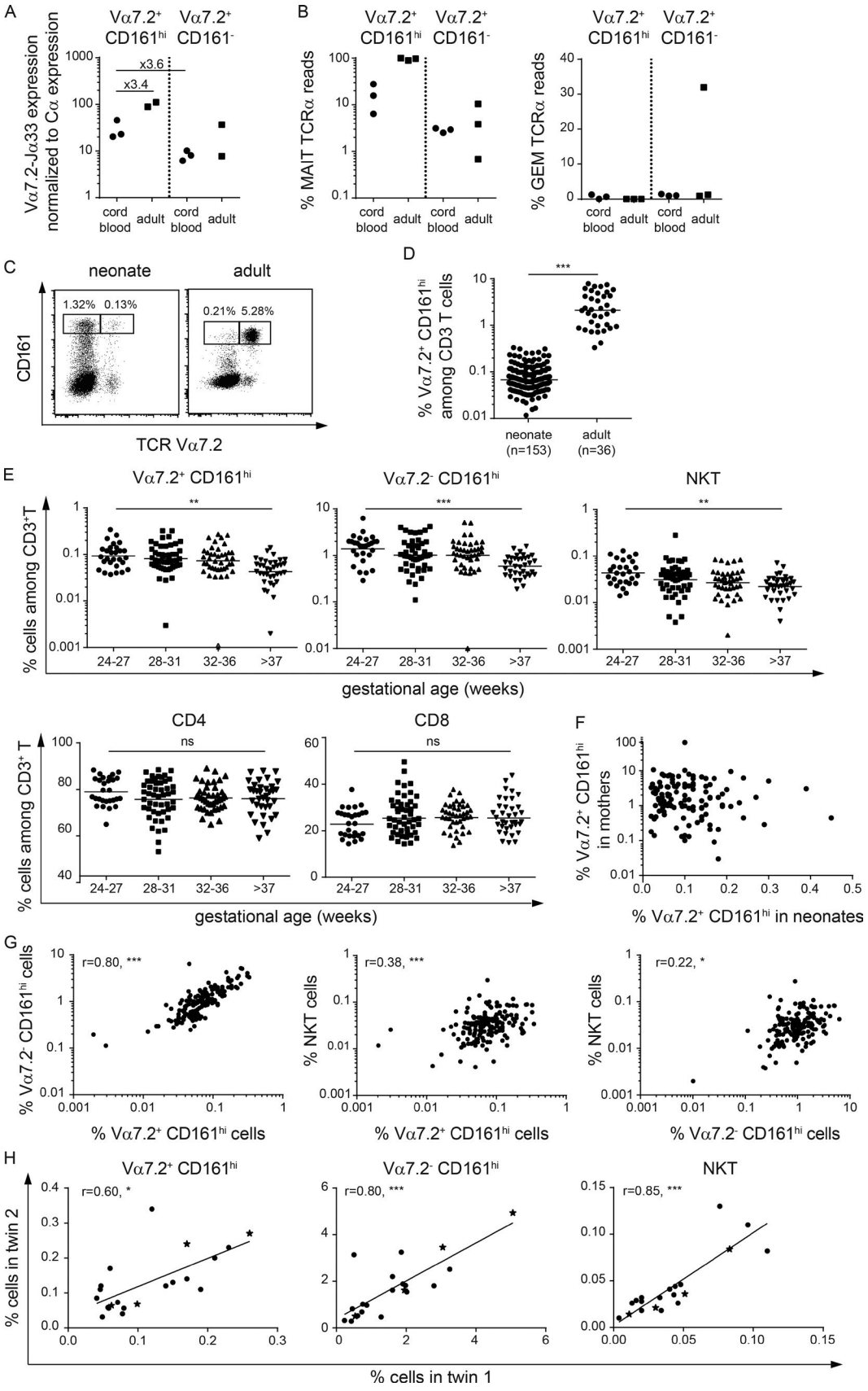
A
Vα7.2+ CD161hi
Vα7.2+ CD161-
Vα7.2-Jα33 expression normalized to Cα expression
x3.6
x3.4
cord blood
adult
B
% MAIT TCRα reads
% GEM TCRα reads
C
neonate
adult
1.32% 0.13%
0.21% 5.28%
CD161
TCR Vα7.2
D
% Vα7.2+ CD161hi among CD3 T cells
neonate (n=153)
adult (n=36)
E
Vα7.2+ CD161hi
Vα7.2- CD161hi
NKT
% cells among CD3+T
24-27
28-31
32-36
>37
gestational age (weeks)
CD4
CD8
ns
F
% Vα7.2+ CD161hi in mothers
% Vα7.2+ CD161hi in neonates
G
% Vα7.2- CD161hi cells
% NKT cells
% Vα7.2+ CD161hi cells
% Vα7.2- CD161hi cells
r=0.80, ***
r=0.38, ***
r=0.22, *
H
r=0.60, *
r=0.80, ***
r=0.85, ***
% cells in twin 2
% cells in twin 1

riched for another recently described conserved Vα7.2$^+$ T cell population, the CD1b-reactive germline-encoded mycolyl lipid-reactive (GEM) T cells characterized by a TRAV1-2 TRAJ9 and 13–amino acid–long CDR3 TCR (Van Rhijn et al., 2013; Fig. 1 B, right).

Altogether, these results indicate that the Vα7.2 and CD161 staining allows identification of circulating stage 3 MAIT cells at birth. However, the Vα7.2$^+$ CD161^{high} fraction in cord blood may also encompass other T cells probably sharing a common developmental pathway (as discussed in Legoux et al. [2017]).

We determined the frequency and absolute numbers of peripheral blood Vα7.2$^+$ CD161^{high} CD3$^+$ CD4$^-$ T cells in a cohort of 153 neonates (born between 24 and 42 wk postconception) admitted at birth in the Neonatology Department. In line with studies in cord blood, the frequency of Vα7.2$^+$ CD161^{high} T cells in newborns was 30 times lower than in healthy adults (mean proportion among CD3$^+$ cells 0.07% and 2.16%, respectively; Fig. 1, C and D). Of note, significant differences were observed when newborns were divided according to gestational age, with extremely preterm babies displaying higher Vα7.2$^+$ CD161^{high} T cell frequencies than term babies (mean in group 1: 0.10%; group 2: 0.08%; group 3: 0.07%; group 4: 0.04%; P for trend = 0.0002; Fig. 1 E). This inverse relationship with gestational age over the 24-to 42-wk span was not observed for conventional αβ T cells (both CD4 and CD8; Fig. 1 E, bottom). The frequency of Vα7.2$^+$ CD161^{high} T cells in neonates was not correlated to that of their mother on the day of delivery (Fig. 1 F).

CD161 expression in CD8 T cells is a marker of type-17 differentiation program and is associated with specific tissue homing properties (Billerbeck et al., 2010; Maggi et al., 2010). Although the CD161^{high} CD8 T cell population is dominated by Vα7.2$^+$ MAIT cells in adult blood, the opposite has been observed in cord blood where Vα7.2$^-$ cells are predominant (Walker et al., 2012). In neonates, Vα7.2$^-$ CD161^{high} T cells were 10 times more abundant than Vα7.2$^+$ CD161^{high} T cells, and their frequency was inversely correlated with gestational age (Fig. 1 E). Moreover, Vα7.2$^+$ and Vα7.2$^-$ CD161^{high} T cell frequencies were strongly correlated (r = 0.80, P < 0.0001), supporting the hypothesis that these two populations have a common prenatal developmental program (Walker et al., 2012; Legoux et al., 2017; Fig. 1 G). NKT cell frequencies were also negatively related to gestational age, but their correlation with Vα7.2$^+$ and Vα7.2$^-$ CD161^{high} T cell frequencies was much weaker (Fig. 1, E and G).

In 21 twin pairs the percentages of Vα7.2$^+$ CD161^{high} T cells were highly correlated between monozygotic, and strikingly also dizygotic twins, at variance with the large variability observed among unrelated neonates. The same correlation was observed for Vα7.2$^-$ CD161^{high} T cells and NKT cells (Fig. 1 H). This suggests that common prenatal environmental factors may control the development of innate-like T cell populations.

Collectively, our results indicate that fetal Vα7.2$^+$ CD161^{high} T cells undergo an early wave of thymic development, in agreement with their presence in the thymus of aborted second-trimester fetuses (Leeansyah et al., 2014). Their decline with gestational age, also observed for Vα7.2$^-$ CD161^{high} and NKT cells, may be related to their recruitment to mucosal tissues at the end of gestation, although there was no correlation between gestational age and Vα7.2$^+$ CD161^{high} T cell frequency in the fetal tissues examined in a previous study (Leeansyah et al., 2014). More likely, this decreased frequency is due to the dilution of innate-like T cells by conventional T cells seeding the periphery, as suggested by the concomitant increase of conventional CD4 and CD8 T lymphocyte absolute numbers (Fig. S1 A).

Postnatal expansion and maturation of Vα7.2$^+$ CD161^{high} T cells

The low frequency of MAIT cells at birth may be related to the absence of microbial-derived MR1-ligands because of the sheltered intrauterine life. The acute transition from the normally sterile intrauterine environment to the postbirth antigen-rich environment (85% of the bacteria colonizing the gut synthesize riboflavin; Mondot et al., 2016), should lead to an expansion of MAIT cells and acquisition of mem-

Figure 1. **Vα7.2$^+$ CD161^{high} T cell frequencies in neonates. (A)** Quantification of the Vα7.2-Jα33 rearrangement (TRAV1-2 TRAJ33) by qPCR. Vα7.2-Jα33 expression was normalized to Cα expression in FACS-sorted Vα7.2$^+$ CD161^{high} and Vα7.2$^+$ CD161$^-$ cells from three cord blood and two adult blood samples. The median from adult blood Vα7.2$^+$ CD161^{high} populations was arbitrarily set to 100%. **(B)** Quantification of the canonical MAIT TCRα reads (TRAV1-2 TRAJ33/20/12 and 12–amino acid–long CDR3; left) and GEM TCRα reads (TRAV1-2 TRAJ9 and 13–amino acid–long CDR3; right) in sorted Vα7.2$^+$ CD161^{high} and Vα7.2$^+$ CD161$^-$ populations from three cord blood and three adult blood samples. **(C)** Representative Vα7.2$^+$ CD161^{high} cell staining in a neonate and a healthy adult control. Numbers indicate the percentage of Vα7.2$^+$ and Vα7.2$^-$ CD161^{high} cells among the CD3$^+$ CD4$^-$ γδ$^-$ T cell gate. **(D)** Statistical dot plots showing the percentage of Vα7.2$^+$ CD161^{high} cells among CD3$^+$ T lymphocytes in 153 neonates and 36 healthy adult controls. Geometric means (horizontal bars) and statistical significance (Mann–Whitney test) are indicated. **(E)** Individual values and geometric means (horizontal bars) of frequencies of Vα7.2$^+$ CD161^{high}, Vα7.2$^-$ CD161^{high}, NKT, and conventional CD4 and CD8 T cells in each group of neonates (GA 24–27 wk, *n* = 28; GA 28–31 wk, *n* = 48; GA 32–36 wk, *n* = 41; >37 wk, *n* = 36). Differences between means were analyzed by one-way ANOVA with posttest for linear trend. **(F)** Correlation between the frequencies of Vα7.2$^+$ CD161^{high} cells in 115 neonates and their mothers at birth. **(G)** Correlation between the frequencies of Vα7.2$^+$ CD161^{high}, Vα7.2$^-$ CD161^{high}, and NKT cells in 153 neonates at birth. The percentage of cells was transformed by using log to base 10 to perform statistical analysis. Spearman rank correlation coefficients (r) are indicated. **(H)** Correlation of the frequencies of Vα7.2$^+$ CD161^{high} cells (left), Vα7.2$^-$ CD161^{high} cells (medium), and NKT cells (right) between 21 twin pairs at birth (4 monozygotic and 17 dizygotic pairs, indicated by asterisks and circles, respectively). *, P < 0.01; **, P < 0.001; ***, P < 0.0001.

ory features in the first weeks of life. Because the number of infants still hospitalized after 1 mo of life was relatively small, we extended our study to 132 additional neonates with gestational age distribution similar to that of the first cohort. As $V\alpha7.2^+$ $CD161^{high}$ T cell frequencies in this replication cohort entirely confirmed those from the first one, the two cohorts were combined hereafter (Fig. S1 B). $V\alpha7.2^+$ $CD161^{high}$ T cell numbers only slightly increased during the first 2 mo of life, remaining much scarcer than in adult blood (Fig. 2 A). $V\alpha7.2^-$ $CD161^{high}$ T and NKT cells did not significantly increase over time, as expected because their numbers in adults are quite similar to those in neonates.

Upon delivery, neonates are rapidly exposed to and colonized by maternal microorganisms whose composition is determined by the type of delivery (vaginal or C-section; Dominguez-Bello et al., 2010). Because microbial colonization plays a major role in MAIT expansion in mice (Martin et al., 2009), we wondered if the mode of delivery had an impact on $V\alpha7.2^+$ $CD161^{high}$ T cell numbers 1 mo after birth (Fig. 2 B). There was no difference in $V\alpha7.2^+$ $CD161^{high}$ (as well as $V\alpha7.2^-$ $CD161^{high}$ and NKT) levels between vaginally and C-section–delivered infants, indicating that the type of microbiota colonizing the baby at birth does not influence early postnatal development of these T cells.

Nonmicrobial environmental factors, such as prolonged exposure to corticosteroid (CS) or vitamin D levels, were previously described as influencing MAIT cell frequencies in adults (Hinks et al., 2015, 2016). Because antenatal CS therapy is recommended in women at risk of imminent preterm birth, we compared $V\alpha7.2^+$ $CD161^{high}$ T cell frequencies in neonates and in their mothers between those receiving or not CS at least 48 h before delivery. There was no effect of such short-term CS treatment either in neonates or in their mothers (Fig. 2 C). Because serum vitamin D levels were not available, we sought to identify whether there was a seasonal pattern in $V\alpha7.2^+$ $CD161^{high}$ T cell frequencies, given the known seasonal variation in vitamin D levels. There was no association between $V\alpha7.2^+$ $CD161^{high}$ T cell frequencies and the month in which neonates were born, suggesting the lack of relation with sunlight exposure of the mother (Fig. 2 D).

In cord blood, MAIT cells are naive ($CD45RA^+/RO^-$) and express the CD8αβ heterodimer, whereas they are mostly memory and express the CD8αα homodimer in adults (Martin et al., 2009; Dusseaux et al., 2011; Walker et al., 2012; Koay et al., 2016). As expected, the vast majority of $V\alpha7.2^+$ $CD161^{high}$ T cells in neonates displayed a naive phenotype and expressed the CD8β chain, regardless of gestational age. Surprisingly, even though $V\alpha7.2^+$ $CD161^{high}$ T cells did not expand much in the early postnatal life, they very rapidly acquired a memory phenotype (Fig. 2 E). As early as 2 mo of age, almost 40% of $V\alpha7.2^+$ $CD161^{high}$ T cells were already CD45RO or CD8αα/$\alpha\beta^{low}$, in sharp contrast to conventional T cells, which were nearly all still naive (mean 5.2% $CD45RO^+$; $P < 0.0001$).

Because we could not follow up the development of $V\alpha7.2^+$ $CD161^{high}$ T cells in neonates after their discharge (i.e., at a maximum of 2 mo of life), we performed a cross-sectional analysis in 79 healthy children aged 10 mo to 17 yr and 50 adults aged 18–50 yr. $V\alpha7.2^+$ $CD161^{high}$ T cell frequencies slowly increased during infancy to reach a plateau around 6 yr of age, extending previous studies in smaller cohorts (Dusseaux et al., 2011; Koay et al., 2016). In contrast, $V\alpha7.2^-$ $CD161^{high}$ T cell percentages remained stable over time (Fig. 2 F).

Collectively, these results indicate that maturation of $V\alpha7.2^+$ $CD161^{high}$ T cells rapidly occurs after birth, whereas their gradual expansion with age is a very slow process.

$V\alpha7.2^+$ $CD161^{high}$ T cell recovery after cord blood transplantation

The progressive maturation of the neonatal immune system after birth shares some similarities with the progressive recovery of the immune cell subsets after allogeneic hematopoietic stem cell transplantation (HSCT) in children. These two clinical settings are characterized by a delayed development of the long-term protective adaptive immunity, associated with high predisposition to severe microbial infections. To study $V\alpha7.2^+$ $CD161^{high}$ T cell recovery after HSCT, we took advantage of a longitudinal study in 17 children who received unrelated cord blood (UCB) transplantation. $V\alpha7.2^+$ $CD161^{high}$ T cells were almost undetectable in the circulation 1 mo after transplantation, indicating that the host's MAIT cells were not resistant to the myeloablative conditioning regimen given before HSCT, despite their expression of the multidrug efflux protein ABCB1 (Dusseaux et al., 2011). Moreover, $V\alpha7.2^+$ $CD161^{high}$ T cell numbers remained extremely low during the 12-mo study period, whereas $V\alpha7.2^-$ $CD161^{high}$ cells, conventional T cells, and B cells progressively increased to reach normal values 9–12 mo after transplantation (Fig. 3 A). Of note, 80% of circulating $V\alpha7.2^+$ $CD161^{high}$ T cells displayed a naive phenotype 1 mo after HSCT, supporting that they represented donor (cord blood)-derived cells transferred with the graft and not host's residual cells. Thereafter, they rapidly acquired memory characteristics, as observed after birth. A rebound in naive $V\alpha7.2^+$ $CD161^{high}$ T cells occurred between 6 and 12 mo after HSCT (mean 42.5% vs. 75.6% $CD45RO^-$; $P = 0.06$), suggesting the emergence of new HSC-derived naive cells recently exiting the thymus (Fig. 3 B). Importantly, the reconstitution profile of $V\alpha7.2^+$ $CD161^{high}$ T cells was not influenced by the occurrence of acute (<100 d after transplant) graft-versus-host disease (aGVHD) or severe microbial infection (Fig. 3 C).

To check whether the lack of recovery of circulating $V\alpha7.2^+$ $CD161^{high}$ T cells could be related to their attraction to inflammatory tissues early after HSCT, we performed immunohistochemical analysis on biopsy samples. In the absence of available MR1 tetramers for in situ staining, we relied on Vα7.2 staining (which also detects other $V\alpha7.2^+$ conventional T cells). In control samples, few $V\alpha7.2^+$ cells were observed in the normal lamina propria, mostly at the bases of the villi and more occasionally at the villus tip and within the ep-

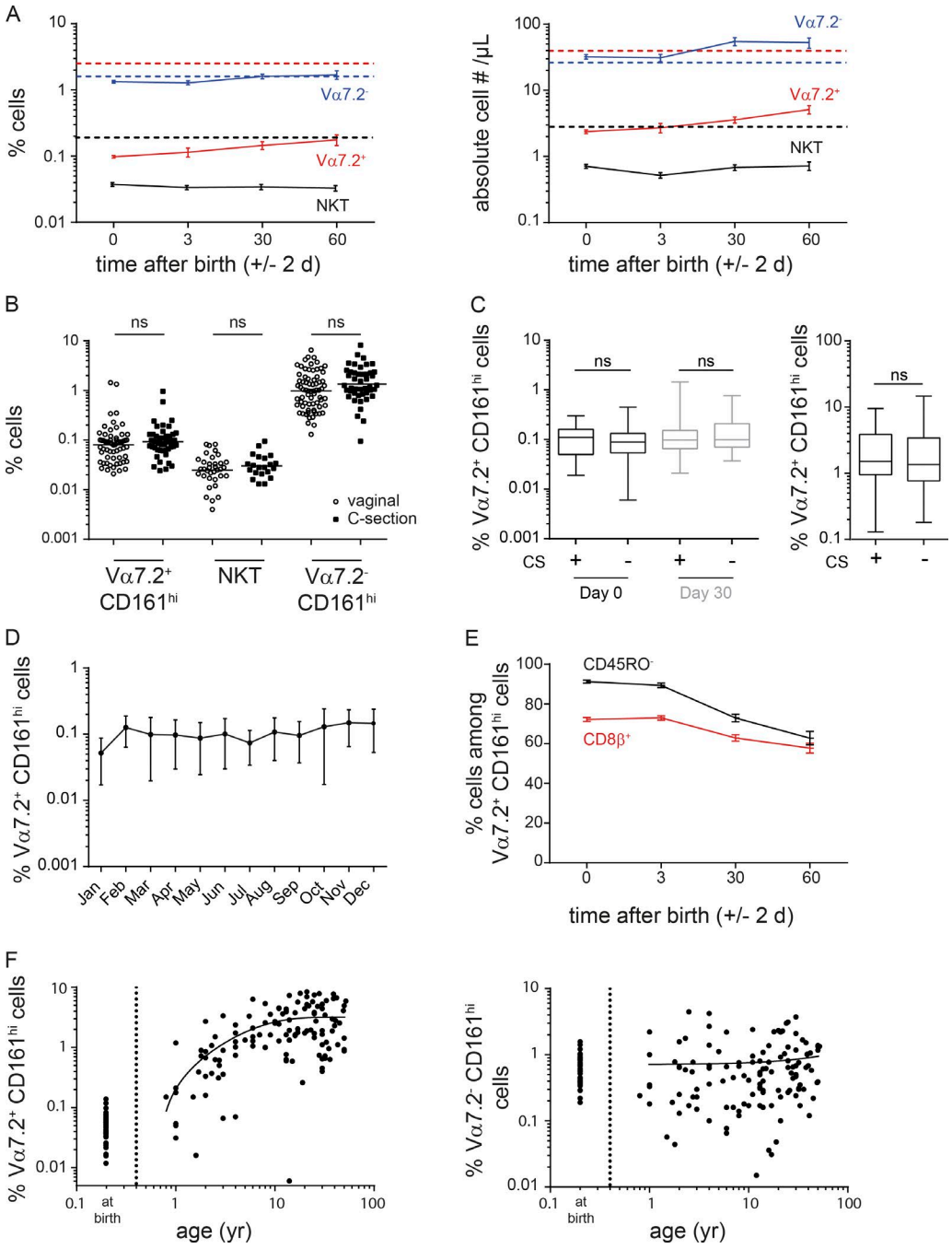

Figure 2. **Kinetics of Vα7.2⁺ CD161^{high} T cell expansion and maturation after birth. (A)** Comparison of Vα7.2⁺ CD161^{high}, Vα7.2⁻ CD161^{high}, and NKT cell expansion after birth in the whole neonate cohort. Results show the mean ± SEM of frequencies (left) and absolute numbers (right) in the indicated populations during the first 2 mo of life. Note that a varying number of subjects was analyzed at the different time points (n = 286 at day 0, n = 186 at day 3, n = 118 at day 30, and n = 49 at day 60) because of drop out (most subjects from groups 3 and 4 were discharged at day 30). Dashed lines represent the mean values in the corresponding population as measured for healthy adults. **(B)** Absence of relationship between percentages of Vα7.2⁺ CD161^{high}, NKT, and Vα7.2⁻ CD161^{high} cells at 1 mo of life and delivery type (vaginal or C-section). Differences between means were analyzed by using the Mann–Whitney unpaired test. **(C)** Effect of antenatal CS therapy on Vα7.2⁺ CD161^{high} T cell frequencies in neonates analyzed at birth and 1 mo of age (left) and in their mothers on the day of delivery (right). Results are depicted as box and whisker plots in the presence (+CS) or absence (-CS) of antenatal CS therapy (two 12-mg intramuscular doses of betamethasone 24 h apart at least 48 h before delivery). **(D)** Absence of variation in neonatal Vα7.2⁺ CD161^{high} T cell frequencies (mean ± SEM) by month of birth. **(E)** Parallel changes in the CD45RO and CD8β Vα7.2⁺ CD161^{high} cell phenotype over the first 2 mo of life in the whole neonate cohort. Results show the mean frequencies ± SEM of

ithelium, as reported (Reantragoon et al., 2013; Fig. 3 D). Vα7.2$^+$ T cells were not found in intestinal lymphoid structures (mesenteric lymph nodes, appendix), except for rare cells in the mantle region of intestinal lymphoid follicles. We next analyzed intestinal biopsies taken for diagnostic purpose (aGVHD vs. viral infection occurring within 3 mo after transplantation). Intestinal aGVHD was assessed by the presence of apoptotic epithelial cells (determined by caspase 3 staining; not depicted). Although large CD3 and CD8 T cell infiltrates were evidenced, no Vα7.2$^+$ lymphocytes were detected in all aGVHD samples examined, whatever the anatomical location (stomach, ileum, colon, rectum) or the intensity/severity of the immune process. Vα7.2$^+$ cells were also undetectable in biopsies from HSCT recipients with documented viral infection or reactivation (CMV, adenovirus, HHV6; Fig. 3 E). Thus, the low recovery of circulating Vα7.2$^+$ CD161^{high} T cells after HSCT is not related to their rapid trafficking to mucosal tissues in response to local inflammatory signals.

To extend our findings beyond 1 yr after transplant, we performed a cross-sectional analysis in 20 additional UCB transplant recipients sampled at the time of a routine hospital visit 1–6 yr after HSCT. Similar to what we observed during infancy, Vα7.2$^+$ CD161^{high} T cell frequencies and absolute numbers progressively increased to reach values observed in healthy, age-matched controls around 5 yr after HSCT (Fig. 3 F).

Collectively, these results indicate that, although effective thymic output may ensure an export of some new naive Vα7.2$^+$ CD161^{high} T cells after UCB transplantation, it does not contribute much to their peripheral expansion, which requires other factors. In mice, the presence of B cells was shown to be necessary for MAIT cell expansion (Martin et al., 2009). As the B cell compartment fully recovered as early as 3 mo after UCB transplantation, it is unlikely that the lack of B cells is responsible for the absence of MAIT expansion in the periphery in this setting.

Relationships between Vα7.2$^+$ CD161^{high} T cells and infections in neonates

Infection is particularly prevalent in early preterm births: chorioamnionitis is implicated in >85% of deliveries occurring before 28 wk of gestation, but the initiating infection may be subclinical (Rubens et al., 2014). We analyzed the potential relationship between microbial infection and peripheral Vα7.2$^+$ CD161^{high} T cell numbers in 51 neonates with early-onset infection. Of note, when infection was microbiologically documented (85% of cases), it usually corresponded to known riboflavin-producing pathogens (*Escherichia coli*, *Candida albicans, Pseudomonas aeruginosa*, group B Streptococcus). Although relative frequencies of Vα7.2$^+$ CD161^{high} T cells at birth were slightly lower in newborns with early-onset infection than in those without infection, their absolute numbers were not different (Fig. 4 A). Moreover, Vα7.2$^+$ CD161^{high} T cell frequencies showed a similar inverse relationship with gestational age in uninfected and infected neonates (Fig. 4 B) and a similar increase during the first 2 mo of life (Fig. 4 C). There was no difference in the Vα7.2$^+$ CD161^{high} T cell maturation profile (CD45RO or CD8β) according to the presence or absence of infection (not depicted).

Extremely preterm neonates in the intensive care unit (ICU) are at high risk of developing infections related to invasive aspects of intensive care. Adult patients with severe nonstreptococcal bacterial infections display an early decrease in MAIT cell count, and the persistence of MAIT depletion is associated with further development of ICU-acquired infections (Grimaldi et al., 2014). We thus analyzed Vα7.2$^+$ CD161^{high} T cell numbers according to the presence or absence of infection acquired during the first 3 wk of life but found no difference (mean absolute number ± SEM at day 60: 3.1 ± 0.8/µl and 2.9 ± 1.5/µl, respectively; NS).

Collectively, these results indicate that neonatal infection is not associated with any changes in peripheral Vα7.2$^+$ CD161^{high} T cell levels or phenotype. In particular, early-onset infection with riboflavin-producing pathogens is not sufficient to induce significant expansion of circulating Vα7.2$^+$ CD161^{high} T cells in the postnatal period.

In fetal and adult tissues, a large proportion of T cells (either Vα7.2$^+$ or Vα7.2$^-$) express high levels of CD161 (Leeansyah et al., 2014; Fergusson et al., 2016), making the identification of MAIT cells difficult in tissues without RT-qPCR or MR1-tetramer staining. Still, the dynamic of Vα7.2$^+$ CD161^{high} T cell accumulation in tissues after birth is not known. We analyzed the frequencies of Vα7.2$^+$ and Vα7.2$^-$ CD161^{high} T cells among mononuclear cells isolated from surgically resected intestinal tissues of different anatomical locations (ileum, colon, rectum) in 16 children aged 1 mo to 16 yr (Fig. 4 D). Whatever the child's age was, Vα7.2$^+$ CD161^{high} T cells were relatively rare within normal intestine (mean percentage of CD3 T cells ± SEM: 0.27 ± 0.06%; n = 8 patients), i.e., at a proportion similar to those reported in fetuses and adults (Leeansyah et al., 2014; Serriari et al., 2014; Sundström et al., 2015; Fergusson et al., 2016). They were barely detectable within appendixes (0.07 ± 0.03%; n = 5 patients). We also analyzed intestinal samples from three neonates with necrotizing enterocolitis, a devastating hyperinflammatory disease that mostly affects preterm newborns and likely results from inappropriate response to gut microbiota (Neu and Walker, 2011). Even in this inflammatory setting, frequencies of Vα7.2$^+$ CD161^{high} T cells were very low. In all intestinal samples, Vα7.2$^-$

CD45RO$^-$ and CD8β$^+$ cells at the different time points. **(F)** Relationship between log10-based transformed Vα7.2$^+$ CD161^{high} cell percentages and age. Results show individual values of Vα7.2$^+$ CD161^{high} and Vα7.2$^-$ CD161^{high} cell frequencies in 79 healthy children aged 10 mo to 17 yr and 50 healthy adults aged 18–50 yr. Values in 36 healthy term neonates are shown for comparison.

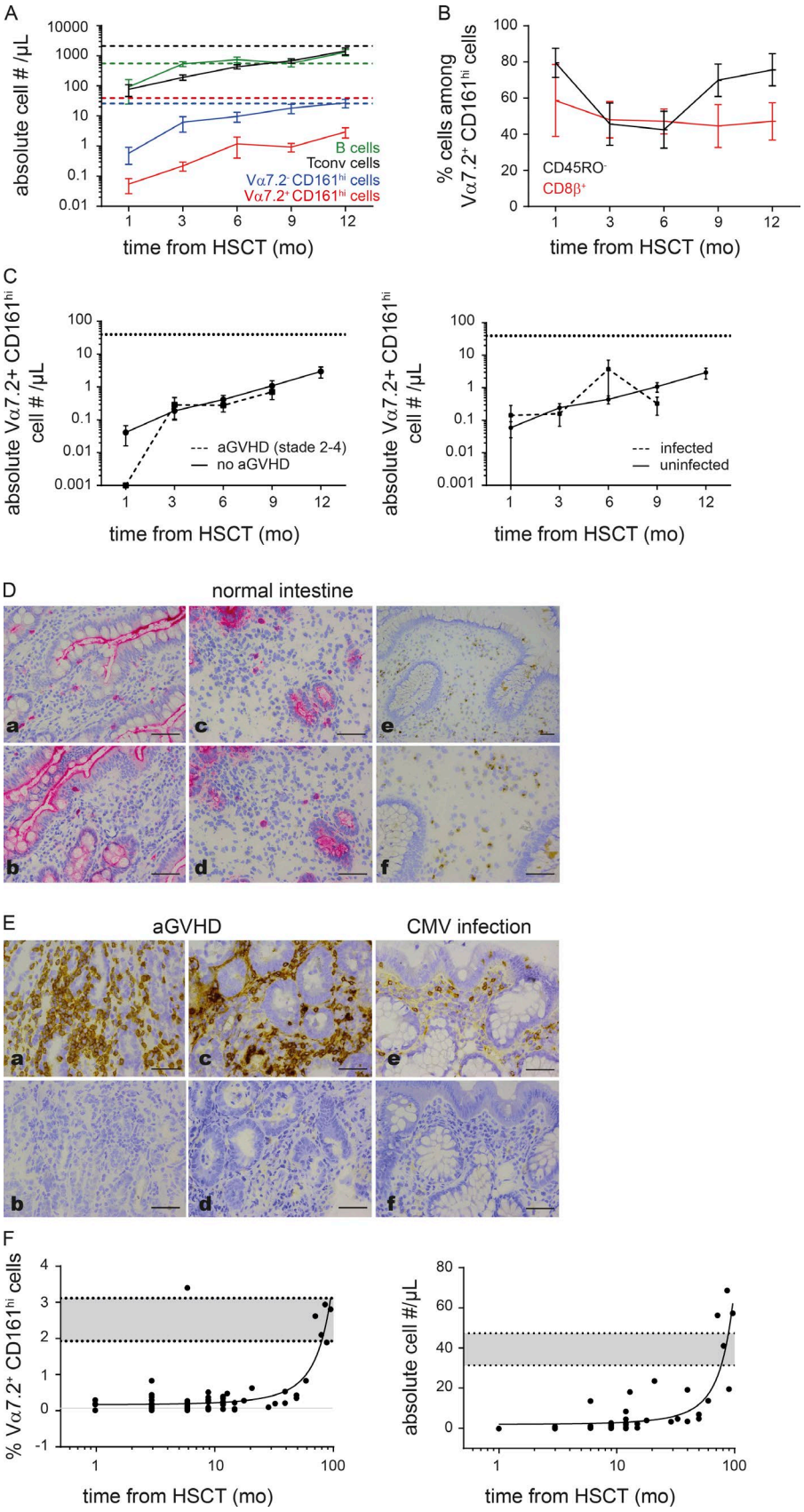

Figure 3. **Vα7.2⁺ CD161^{high} T cell recovery and maturation after unrelated cord blood transplantation in children. (A)** Recovery dynamics of Vα7.2⁺ CD161^{high}, Vα7.2⁻ CD161^{high}, and conventional T and B cells during the first 12 mo after UCB transplantation (n = 17 children). Data are depicted as the mean absolute values ± SEM. Dashed lines represent the mean values in the corresponding population as measured for healthy, age-matched children (n = 75). **(B)** Parallel changes in the CD45RO and CD8β Vα7.2⁺ CD161^{high} cell phenotype during the first 12 mo after UCB transplantation. Results show the mean frequencies ± SEM of CD45RO⁻ and CD8β⁺ cells at the different time points. The rebound in CD45RO⁻ MAIT numbers around 9 mo after HSCT (P = 0.06 compared with values at 6 mo) coincides with the emergence of newly thymus-derived naive cells. **(C)** Recovery dynamics of Vα7.2⁺ CD161^{high} T cells according to the presence or absence of aGVHD (left) or severe microbial infection (right). **(D)** Immunohistochemical staining of intestinal tissue sections from normal small intestine samples showing the presence of CD8⁺ (panels a and c) and Vα7.2⁺ (panels b and d–f) cells. Staining is detected with AP- (panels a–d) or HRP (panels e and f)-antibody conjugate. Bars, 50 µm. **(E)** Immunohistochemical staining of intestinal biopsies taken for diagnostic purpose of aGVHD (panels a–d) or CMV infection (panels e and f) in HSCT children recipients, showing the presence of CD3⁺ (panel a) and CD8⁺ (panels c and e) cells but the absence of Vα7.2⁺ (panels b, d, and f) cells. Staining is detected with HRP-antibody conjugate. Bars, 50 µm. **(F)** Relationship between Vα7.2⁺ CD161^{high} cell percentages (left) or absolute numbers (right) and time from transplantation in 36 cord blood transplant children recipients. Dashed lines represent the 95% confidence interval as measured for healthy, age-matched controls.

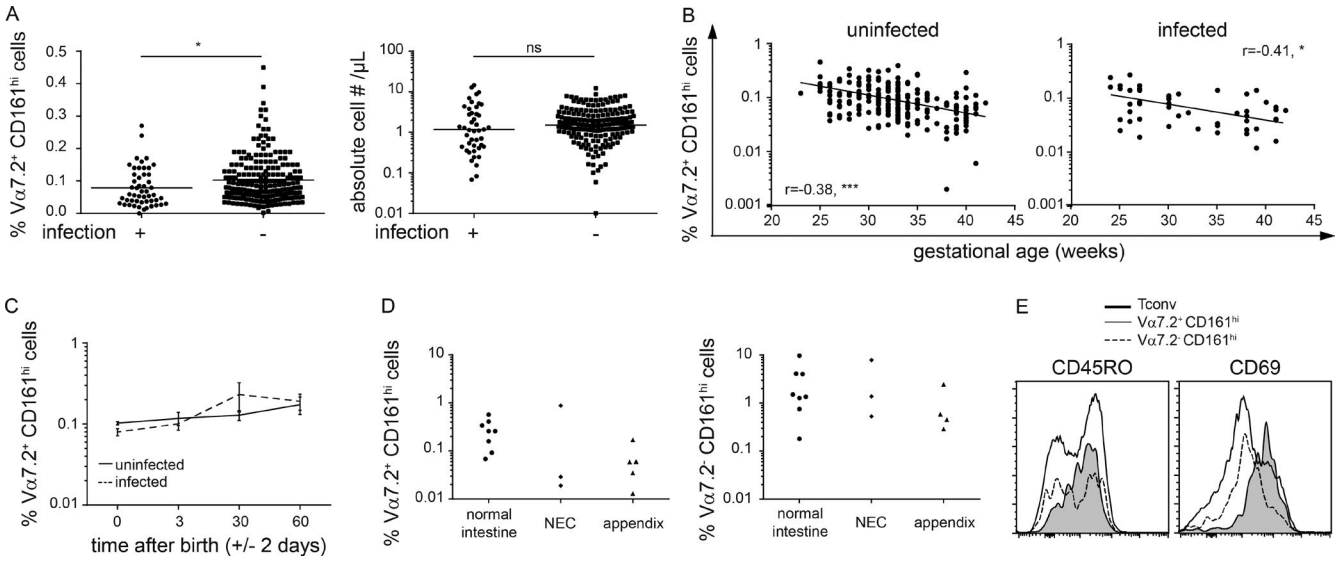

Figure 4. **Relationships between Vα7.2⁺ CD161^{high} T cells and early-onset infection in neonates. (A)** Individual values and means (horizontal bars) of Vα7.2⁺ CD161^{high} T cell frequencies (left) and absolute numbers (right) at birth in extremely preterm neonates with (+) and without (–) early-onset infection. Differences between means were analyzed by using Mann–Whitney unpaired test. **(B)** Relationship between log10-based transformed Vα7.2⁺ CD161^{high} cell percentages at birth and gestational age over the 24- to 42-wk span in the absence (left) or presence (right) of early-onset infection. Spearman rank correlation coefficients (r) and P values are indicated. **(C)** Kinetics of Vα7.2⁺ CD161^{high} cell expansion during the first 2 mo of life in neonates with and without early-onset infection. Results show the mean percentage ± SEM of Vα7.2⁺ CD161^{high} cells over time and P value (two-way ANOVA). A varying number of subjects was analyzed at the different time points (n = 285 at day 0, n = 285 at day 3, n = 118 at day 30, and n = 49 at day 60) because of drop out. **(D)** Frequencies of Vα7.2⁺ CD161^{high} (left) and Vα7.2⁻ CD161^{high} (right) cells among CD3 T cells isolated from surgically resected normal intestine (n = 8), necrotizing enterocolitis (n = 3), and appendix (n = 5) samples. **(E)** Representative histograms of CD45RO and CD69 expression in Vα7.2⁺ CD161^{high} cells (shaded gray), Vα7.2⁻ CD161^{high} cells (dotted line), and conventional T cells (black line) isolated from a normal intestinal sample in a 2-mo-old child. *, P < 0.01; ***, P < 0.0001.

CD161^{high} T cells were 10 times more abundant than Vα7.2⁺ CD161^{high} T cells (Fig. 4 D).

In contrast with thymic and cord blood cells, Vα7.2⁺ CD161^{high} T cells express a memory (CD45RO⁺) phenotype in fetal mucosae (Leeansyah et al., 2014). Similarly, in intestinal samples, most Vα7.2⁺ CD161^{high} T cells expressed CD45RO (mean 91% CD45RO⁺) and high levels of CD69, a marker of tissue-resident memory T cells (Sathaliyawala et al., 2013; Thome et al., 2014; 70–100% being CD69⁺; Fig. 4 E). Conversely, only a fraction of Vα7.2⁻ CD161^{high} and conventional T cells expressed a memory phenotype, in agreement with recent data in mucosal tissues from pediatric organ donors (Thome et al., 2016).

Phenotype and functional capacities of peripheral Vα7.2⁺ CD161^{high} T cells

The very low expansion of Vα7.2⁺ CD161^{high} T cells after birth or cord blood transplantation may be related to cell intrinsic characteristics or to limited availability of microbial-derived MR1-ligands. We first examined if the expansion of peripheral neonatal Vα7.2⁺ CD161^{high} T cells was restricted by selective cytokine responsiveness. We found similar prominent expression of IL-18Rα and IL-7Rα in cord blood and adult Vα7.2⁺ CD161^{high} T cells. Expression of IL-12Rβ2 and IL-23R was much lower but again comparable in cord blood and adult cells (Fig. 5 A). This suggests that the low expansion of naive Vα7.2⁺ CD161^{high} T cells after birth or after HSCT is not related to hyporesponsiveness to innate or homeostatic cytokines.

The PLZF transcription factor is considered a master regulator of innate-like T cell development and maturation, including NKT and γδ T cells (Kovalovsky et al., 2008; Savage et al., 2008). A gradual acquisition of PLZF expression occurs between stage 2 and stage 3 MAIT cells in the thymus (Koay et al., 2016) and continues during postthymic maturation of MAIT cells in peripheral blood (Cui et al., 2015; Rahimpour et al., 2015). We found that naive cord blood Vα7.2⁺ CD161^{high} T cells expressed significantly lower levels of PLZF than adult ones (Fig. 5 B), suggesting that final maturation of cord blood Vα7.2⁺ CD161^{high} T cells requires an early activation signal after birth. Notably, a significant proportion of naive cord blood Vα7.2⁺ CD161^{high} T cells expressed measurable level of CD25 (Fig. 5 B), and PLZF levels were significantly higher in CD25-positive cells than in CD25-negative cells (Fig. 5 C). This may be related to a low level of stimulation by microbial antigen already available at birth, as also suggested by the higher proportion of cycling cells in cord blood Vα7.2⁺ CD161^{high} T cells in comparison with adult ones (mean Ki67 expression: 4% vs. 0.65%; Fig. 5 D).

Adult MAIT cells are hypoproliferative in vitro compared with other T cell subsets (Dusseaux et al., 2011; Turtle et

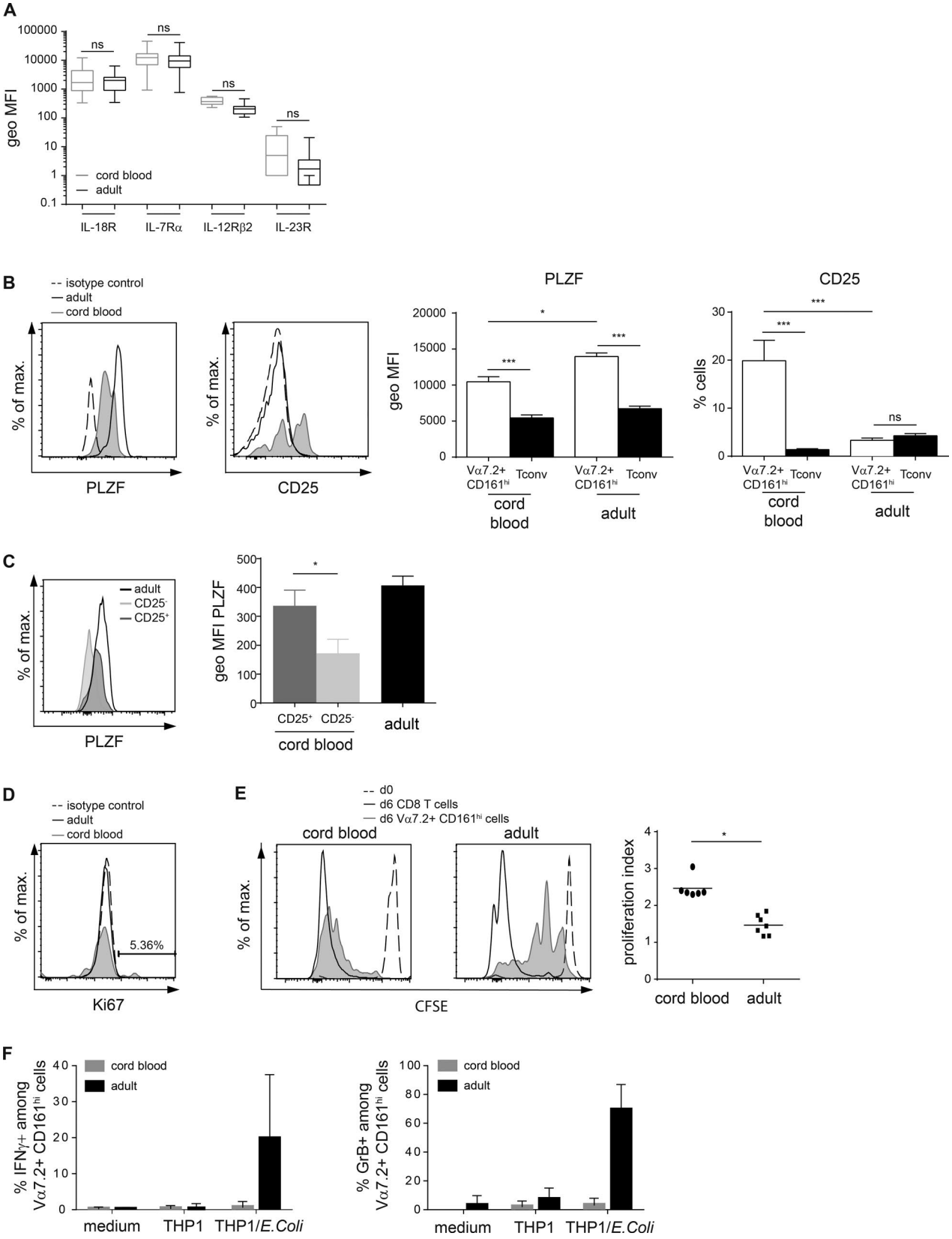
A
geo MFI
100000
10000
1000
100
10
1
0.1
ns
cord blood
adult
IL-18R
IL-7Rα
IL-12Rβ2
IL-23R
B
-- isotype control
adult
cord blood
% of max.
PLZF
CD25
PLZF
CD25
geo MFI
% cells
Vα7.2+ CD161hi
Tconv
cord blood
adult
C
adult
CD25-
CD25+
% of max.
PLZF
geo MFI PLZF
CD25+
CD25-
cord blood
adult
D
-- isotype control
adult
cord blood
% of max.
5.36%
Ki67
E
-- d0
d6 CD8 T cells
d6 Vα7.2+ CD161hi cells
cord blood
adult
% of max.
CFSE
proliferation index
F
% IFNγ+ among Vα7.2+ CD161hi cells
% GrB+ among Vα7.2+ CD161hi cells
cord blood
adult
medium
THP1
THP1/E.Coli

al., 2011). To assess the intrinsic proliferative capacity of cord blood Vα7.2$^+$ CD161^{high} T cells, we analyzed their in vitro proliferation in response to mitogen. As indicated by the high proportion of CFSE^{low} cells, cord blood Vα7.2$^+$ CD161^{high} T cells strongly proliferated after 6-d PHA stimulation, similarly to conventional CD8 T cells. Adult Vα7.2$^+$ CD161^{high} T cells proliferated much less efficiently (Fig. 5 E).

Finally, we investigated the ability of cord blood Vα7.2$^+$ CD161^{high} T cells to respond to short-term stimulation with microbial MR1 ligands. Magnetic bead-enriched CD4$^-$ T cells were incubated overnight in the presence of MR1-expressing THP1 cells loaded with paraformaldehyde-fixed *E. coli*, and IFNγ and Granzyme B (GrB) production was assessed in Vα7.2$^+$ CD161^{hi} cells. *E. coli* clearly induced intracellular accumulation of IFNγ and GrB in adult Vα7.2$^+$ CD161^{high} T cells, but not in cord blood cells (Fig. 5 F), in line with their naive phenotype. Longer *E. coli* stimulation (up to 5 d) induced a high mortality of cord blood Vα7.2$^+$ CD161^{high} T cells. Overnight stimulation by IL-12 and IL-18 combination was also unable to stimulate cord blood cells (not depicted). Thus, in contrast to mature MAIT cells in adult blood, cord blood Vα7.2$^+$ CD161^{high} T cells are not able to display immediate effector functions toward bacterially infected cells. These data indicate that, although they have intrinsic ability to proliferate, cord blood Vα7.2$^+$ CD161^{high} T cells need functional maturation and/or expansion after birth to acquire detectable effector activities after microbe-derived antigen recognition.

TCR repertoire of Vα7.2$^+$ CD161^{high} MR1:5-OP-RU tetramer$^{pos/neg}$ T cells in cord blood

As the MR1:5-OP-RU tetramer became available during the course of this study (National Institutes of Health [NIH] tetramer core facility), we determined how the Vα7.2$^+$ CD161^{high} and MR1:5-OP-RU tetramer$^{pos/neg}$ populations overlap. More than 92% of Vα7.2$^+$ CD161^{high} cells were stained with the MR1:5-OP-RU tetramer in adult blood, in contrast with only 2–15% in cord blood (Fig. 6 A), in line with previous results (Eckle et al., 2014; Koay et al., 2016).

We further characterized the α chain of these populations by deep sequencing and found that the Vα7.2$^+$ CD161^{high} tetramer^{pos} subset in cord blood was highly enriched in the canonical MAIT TCR α chain compared with the tetramer^{neg} subset (Fig. 6 B). Yet, the canonical MAIT TCR α chains were more frequent in the Vα7.2$^+$ CD161^{high} tetramer^{neg} than in the Vα7.2$^+$ CD161$^-$ population. These results fully support our initial analysis of the TCR α chain in cord blood subsets (Fig. 1 A). Altogether, they suggest that the CD161^{high} phenotype in cord blood Vα7.2$^+$ T cells delineates a subset of cells enriched in the canonical MAIT TCR α chain, with only a part reactive to 5-OP-RU presented by MR1, certainly according to the fine specificity imparted by the TCR β chain. It is likely that these few clones then expand to form the adult MAIT pool because almost all Vα7.2$^+$ CD161^{high} cells in adult blood express the canonical MAIT TCR and are stained by the MR1:5-OP-RU tetramer.

We therefore studied peripheral blood samples from 83 healthy infants aged from 1 d to 12 mo and found that the proportion of MR1:5-OP-RU tetramer^{pos} cells increased very rapidly, representing already more than 50% of Vα7.2$^+$ CD161^{high} cells at 1 mo of life and the vast majority at 6 mo (Fig. 6 C). Conversely, MR1:5-OP-RU tetramer^{neg} cells tended to disappear (Fig. S2). Moreover at 1 mo, more than 80% of tetramer^{pos} cells already expressed a mature phenotype, whereas maturation of Vα7.2$^+$ CD161^{high} tetramer^{neg} cells was delayed (20% at 1 mo, 80% at 7 mo). Reduction in CD8β expression was concomitant to the acquisition of CD45RO. In addition, from 3–4 wk of age, an important proportion of Vα7.2$^+$ CD161^{high} tetramer^{pos} (but not tetramer^{neg}) cells expressed CD69, suggesting a recent activation in vivo (Fig. 6 D).

Altogether, these results indicate that expansion and maturation of the tetramer^{pos} cells within the Vα7.2$^+$ CD161^{high} population occurs in the first days after birth, suggesting the presence of some 5-OP-RU ligand providing an early maturation signal. This signal is likely not quantitatively sufficient to drive significant expansion of peripheral blood MAIT cells, which remain in very low amounts at this stage.

Figure 5. **Phenotype and functional characteristics of neonatal Vα7.2$^+$ CD161^{high} T cells.** Lymphocytes were isolated from 6–10 cord blood samples from full-term healthy neonates and the same number of healthy adult donors. **(A)** Expression levels of the indicated cytokine receptors. Box and whisker plot shows median, interquartile range, and the 10th and the 90th percentiles of geometric mean fluorescence intensity (MFI; Mann-Whitney test). **(B)** Left: Representative histograms of PLZF and CD25 expression by cord blood and adult blood Vα7.2$^+$ CD161^{high} T cells. Right: Mean values ± SEM of PLZF and CD25 expression by Vα7.2$^+$ CD161^{high} cells and conventional T cells from cord blood and adult blood (Mann–Whitney test). **(C)** Left: Representative histogram of PLZF expression in CD25$^+$ and CD25$^-$ cord blood Vα7.2$^+$ CD161^{high} T cells and adult blood cells. Right: Mean values ± SEM of PLZF expression by CD25$^+$ and CD25$^-$ Vα7.2$^+$ CD161^{high} cord blood cells (paired *t* test) and adult blood Vα7.2$^+$ CD161^{high} cells. Data were not acquired on the same flow cytometer as those in B, so MFI values cannot be compared. **(D)** Representative Ki67 intracellular staining in freshly isolated Vα7.2$^+$ CD161^{high} cells from cord blood (shaded gray) and adult blood (black) samples. The percentage of cycling Vα7.2$^+$ CD161^{high} cells, estimated by the fraction of Ki67$^+$ cells, in the cord blood sample is indicated. **(E)** Vα7.2$^+$ CD161^{high} cell proliferating capacity. Left: Representative CFSE staining gated on Vα7.2$^+$ CD161^{high} T cells (shaded gray) and conventional CD8 T cells (black line) from cord blood and adult blood after 6-d culture with PHA. Dashed histogram shows the basal CFSE staining at day 0. Right: Individual values and means (horizontal bars) of proliferation index in response to PHA in cord blood and adult blood Vα7.2$^+$ CD161^{high} cells. P-value (Mann–Whitney test) is indicated. **(F)** Vα7.2$^+$ CD161^{high} T cell responses to microbial MR1 ligands. Freshly isolated CD4-negative T cells were cultured overnight in the presence or absence of THP-1/*E. coli* or THP-1 alone as negative control, at a 1:1 THP1/CD8 T cell ratio. Intracellular accumulation of IFNγ (left) and GrB (right) in Vα7.2$^+$ CD161^{high} cells from cord blood or healthy adult control was evaluated by flow cytometry. *, $P < 0.01$; ***, $P < 0.0001$.

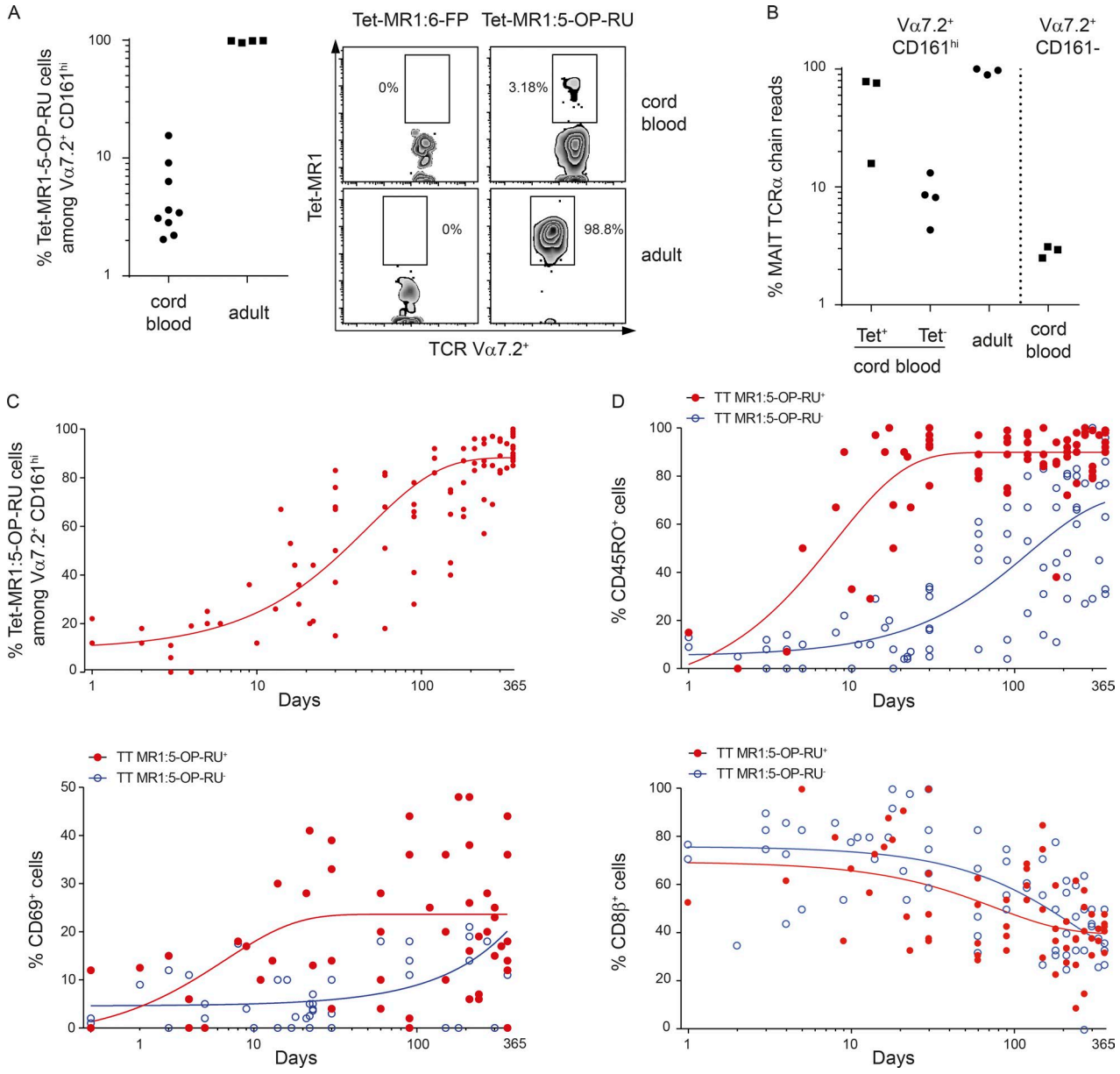

Figure 6. **Postnatal expansion of Vα7.2$^+$ CD161^{high} MR1:5-OP-RU tetramer^{pos} and tetramer^{neg} cells. (A)** Identification of MR1:5-OP-RU reactive cells. Left: Dot plots showing the percentages of MR1:5-OP-RU tetramer^{pos} cells among CD3$^+$ CD4$^-$ Vα7.2$^+$ CD161^{high} cells in nine cord blood and four healthy adult blood samples. Right: Representative staining with MR1:6-FP tetramer (negative control, left quadrants) or MR1:5-OP-RU tetramer (right quadrants) in a cord blood and a healthy adult control. Numbers indicate the percentage of tetramer^{pos} cells among the CD3$^+$ CD4$^-$ Vα7.2$^+$ CD161^{high} T cell gate. **(B)** Percentage of canonical MAIT TCRα chain (as in Fig. 1 B) reads among FACS-sorted MR1:5-OP-RU tetramer^{pos}, tetramer^{neg}, or total CD3$^+$ CD4$^-$ Vα7.2$^+$ CD161^{high} cells from cord blood and a healthy adult and Vα7.2$^+$ CD161$^-$ from cord blood (negative control). **(C)** The proportion of MR1:5-OP-RU tetramer^{pos} cells among CD3$^+$ CD4$^-$ Vα7.2$^+$ CD161^{high} cells rapidly increases with age. Results show individual values in 79 healthy children aged 1 to 360 d. **(D)** Maturation (CD45RO and CD8β) and activation (CD69) phenotype of MR1:5-OP-RU tetramer^{pos} (red dots) and tetramer^{neg} (blue dots) cells among CD3$^+$ CD4$^-$ Vα7.2$^+$ CD161^{high} cells in relation with age.

To verify our hypothesis that the fine specificity of the TCR conferred by the β chain must be important for 5-OP-RU recognition and cell expansion, we studied TCR β chain repertoire of adult and cord blood subsets. Adult MAIT cells display oligoclonal expansions with high clonal size and biased TRBV usage (Tilloy et al., 1999; Lepore et al., 2014). Although cord blood MAIT cells display a diverse repertoire as studied with anti-Vβ antibodies (Walker et al., 2012), no extensive molecular characterization of their TRBV repertoire has been performed so far. Using 5′ rapid amplifica-

tion of cDNA ends (RACE) technique followed by deep sequencing, we characterized the repertoire of FACS-sorted cord blood Vα7.2$^+$ CD161^{high} T cells in comparison to other cord blood CD8 T cell subsets (Vα7.2$^-$ CD161^{high}, Vα7.2$^+$ CD161$^-$, Vα7.2$^-$ CD161$^-$) and to the same subsets in adult blood. Importantly, memory (CD45RO$^+$) subsets were sorted in adult blood, to allow a meaningful comparison with adult MAIT cells, which are all memory. The rarefaction curves of different subsets, which represent cumulative frequency of individual clonotypes ranked by decreasing frequency, were compared (Fig. 7 A). For cord blood subsets, the curves were straight and overlapping, indicating similar high diversity between the subsets. From cell dilution experiments, we estimated the 5′RACE template exchange efficacy during the reverse transcription step at ∼1–2% (not depicted). Because only 3,000 cells from cord blood were studied, the 30–60 clones making up 80–90% of the reads indicate that all the T cell expressed a different TCR. Identical results were obtained for four cord blood donors (Fig. S3). In contrast, although 10 times as many cells (35,000) were studied, adult MAIT cells encompassed oligoclonal expansions with less than 10 clones making up to 80% of the reads. Albeit less strikingly than in the donor depicted in Fig. 7 A, adult MAIT cells harbored similar oligoclonal expansions in the 13 donors studied (Fig. S3), in line with previous data (Tilloy et al., 1999; Lepore et al., 2014). In many cases, the oligoclonality of MAIT cells was similar to that of the other subsets, certainly because only memory (CD45RO$^+$) CD8$^+$ T cells were included in our sorting, contrary to a previous study (Lepore et al., 2014), and memory CD8 T cells are known to include oligoclonal expansions (Hingorani et al., 1993).

We then assessed whether cord blood and adult blood Vα7.2$^+$ CD161^{high} T cells displayed similar biases in the TCR β chain repertoire. TRBV and TRBJ biases were conserved between donors, excluding a stochastic process. We observed preferential usage of TRBV 4.3, 6.4, 15, and 20.1 and TRBJ 2.6 and lower usage of TRBV 4.1 and 5.1 and TRBJ 1.2 in adult MAIT cells in comparison with both other memory adult CD8 T cell subsets (not depicted) and cord blood Vα7.2$^+$ CD161^{high} (Fig. S4, summarized in Fig. 7 B, left panel for TRBV, right panel for TRBJ). Importantly, no such TRBV or TRBJ usage bias was observed for cord blood Vα7.2$^+$ CD161^{high} in comparison with other cord blood CD8 subsets (Fig. S5), suggesting that the TRBV bias observed in adult MAIT cells is not related to a pairing problem. However, when comparing cord blood Vα7.2$^+$ CD161^{high} MR1:5-OP-RU tetramer^{pos} and tetramer^{neg} subsets (Fig. 7 C), similar to adult MAIT cells, we observed that cord blood MR1:5-OP-RU tetramer^{pos} population tended to express less TRBV4.1, TRBV5.1, and TRBJ1.2 as well as more TRBV6.4 compared with the MR1:5-OP-RU tetramer^{neg} population. No similar biases between cord blood MR1:5-OP-RU tetramer^{pos} and adult MAIT cells were observed for the other segments, but this is probably related to a lack of experimental power because of the very low number of cells studied for the tetramer-positive subset (50 cells). Altogether, these data indicate that the fine specificity of the TCRβ chain is involved in MR1:5-OP-RU complex recognition in accordance with structural data (Eckle et al., 2014).

DISCUSSION

Here, by combining flow cytometry, deep sequencing, and further MR1:5-OP-RU tetramer staining, we decipher the postnatal development of human MAIT cells and other Vα7.2$^+$ and Vα7.2$^-$ CD161^{high} subsets. We longitudinally characterize the maturation and expansion of these populations in infancy and after cord blood transplantation, two clinical settings sharing some similarities for establishment of mature protective immunity. The remarkably superimposable results observed in these two situations allow us to provide a new view of MAIT cell ontogeny in the human.

We characterize three distinct human CD3$^+$ CD4$^-$ CD161^{high} populations present at birth: (1) a subset of Vα7.2$^+$ cells enriched in the canonical MAIT TCR α chain, among which a fraction is reactive to 5-OP-RU presented by MR1 (possibly as a result of the β chain usage), is the naive counterpart of mature MAIT cells found in adult blood and corresponds to the recently described stage 3 MAIT cells that just exit the thymus (Koay et al., 2016); (2) a subset of Vα7.2$^+$ cells not reactive to 5-OP-RU presented by MR1, which predominate at birth but are rapidly outnumbered by MR1:5-OP-RU reactive cells; (3) an abundant subset of Vα7.2$^-$ cells, the proportion of which remain stable over time. These three populations are already present at midgestation as observed in the cord blood of high-preterm neonates, in line with their presence in the thymus of aborted second-trimester fetuses (Leeansyah et al., 2014). These Vα7.2$^+$ and Vα7.2$^-$ CD161^{high} populations likely share a common prenatal developmental program, as suggested by the strong correlation we observe between their frequencies at birth. Moreover, their percentages are highly similar in both monozygotic or dizygotic twin pairs, suggesting that prenatal environmental factors may also control their development. Although it is highly probable that CD161^{high} cells expressing the canonical MAIT TCR are selected on MR1 expressed by double-positive thymocytes, the cell type and molecule selecting CD161^{high} cells that do not express the canonical MAIT TCR remain elusive.

At birth, Vα7.2$^+$ CD161^{high} cells exhibit a naive phenotype and intermediate PLZF levels. Accordingly, they are unable to rapidly produce cytokines or cytotoxic molecules in response to bacterial ligands, in contrast with mature adult MAIT cells. Neither do they respond to stimulation by exogenous IL-12 and IL-18, despite high expression of the receptors for these cytokines. Strikingly, although they represent a minor proportion of Vα7.2$^+$ CD161^{high} cells at birth, MR1:5-OP-RU tetramer^{pos} cells very rapidly predominate over tetramer^{neg} cells. By the age of 6 mo, almost all Vα7.2$^+$ CD161^{high} T cells are MR1:5-OP-RU-reactive MAIT cells. Therefore, the term MAIT cells can be confidently assigned to Vα7.2$^+$ CD161^{high} CD4$^-$ T cells from

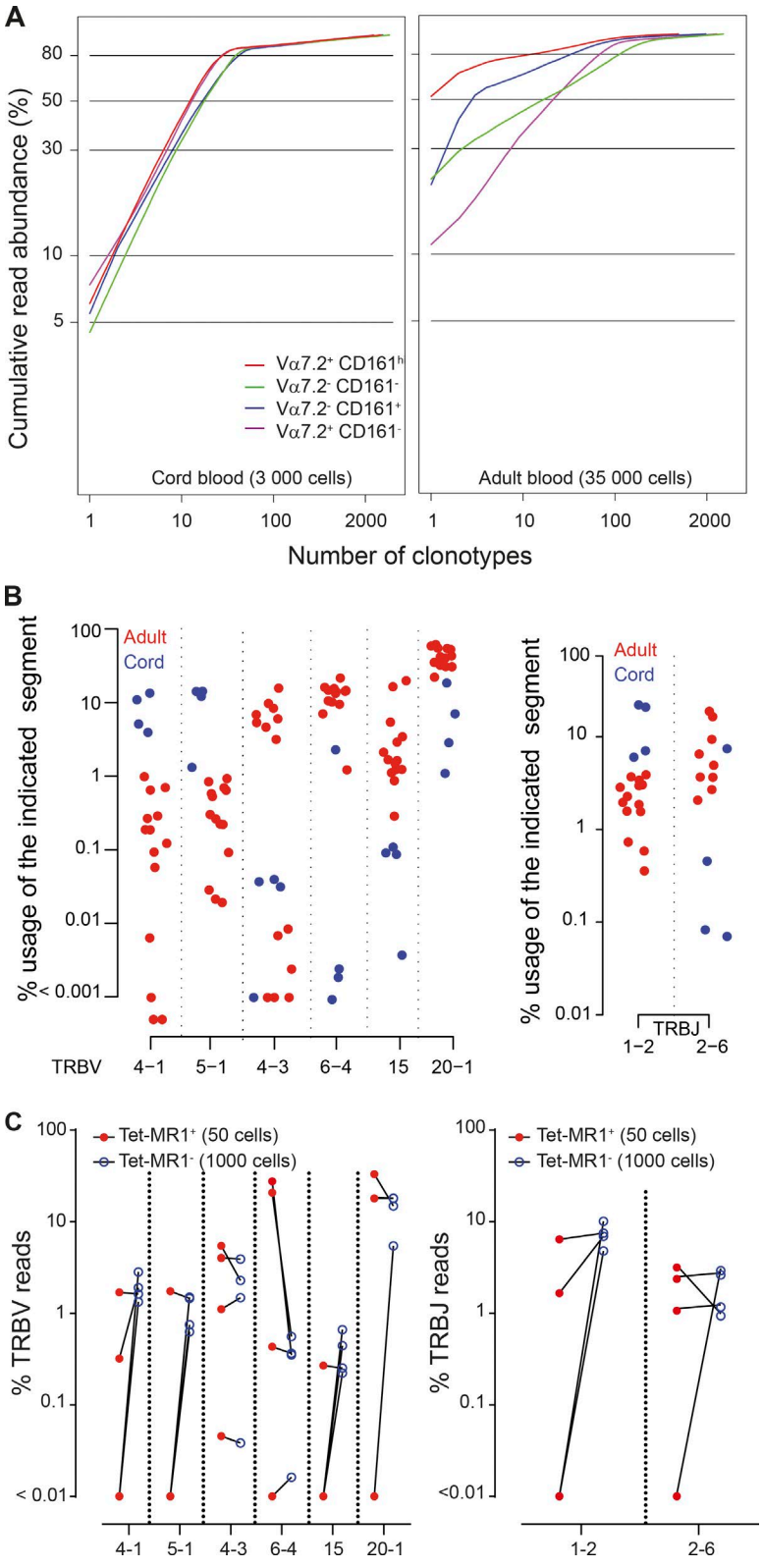

Figure 7. **TCRβ repertoire analysis of cord blood and adult blood MAIT cells. (A)** The analysis was performed by 5′RACE-PCR of sorted T cell subsets. Examples of rarefaction curves from the indicated subsets in cord blood (left) and adult (right) samples. The cumulative frequency of productive TCRβ rearrangement is plotted for individual clonotypes ranked according to decreasing frequency. In adult blood, only memory ($CD45RO^+$) subsets were studied to allow a fair comparison. **(B)** Comparison of the TRBV and TRBJ fragments usage in sorted $CD3^+$ $CD4^-$ $V\alpha7.2^+$ $CD161^{high}$ cells from 4 cord blood (blue) and 14 adult blood (red) samples. Only the Vβ (left) and Jβ (right) genes in which differential expression between neonates and adult samples was found are plotted. The whole dataset is plotted in Fig. S3. **(C)** Comparison of the TRBV (left) and TRBJ (right) gene usage (same segments as in B) in sorted $V\alpha7.2^+$ $CD161^{high}$ MR1:5-OP-RU $tetramer^{pos}$ and $tetramer^{neg}$ cells from four cord blood samples. The analysis was performed by multiplex PCR followed by high-throughput sequencing.

the age of 6 mo after birth (or after HSCT), a crucial point for previous or further human studies conducted in the absence of MR1 tetramer identification.

Importantly, this complete shift in the proportion of $tetramer^{pos}$ MAIT cells within the $V\alpha7.2^+$ $CD161^{high}$ pool is concomitant with their activation ($CD69^+$) and maturation

(CD45RO$^+$). It is likely that colonization by the commensal microbiota provides a key early activation signal, as supported by the impaired development and maturation of MAIT cells in germ-free mice compared with specific pathogen–free mice (Martin et al., 2009; Koay et al., 2016). Whether MAIT cell maturation in the early postnatal period is correlated with the gut microbiota diversity or function (availability of riboflavin metabolites) is currently under investigation in our laboratory. However, although microbe-mediated expansion of peripheral MAIT cells was demonstrated in mouse infection models (Meierovics et al., 2013; Chen et al., 2017), early- or late-onset neonatal microbial infection is not sufficient to induce a significant expansion in circulating MAIT cells. Indeed, MAIT cells very slowly populate the periphery during infancy, taking ∼5–6 yr to achieve adult levels. This gradual process, observed both in childhood and after cord blood transplantation, is not related to a MAIT-cell intrinsic proliferative defect. Rather, it may reflect specific requirements to allow for continuous proliferation, such as repeated exposure to pathogenic bacteria that provide more than single TCR/MR1:ligand interactions. In mice, administration of synthetic 5-OP-RU alone causes CD69 up-regulation but does not result in MAIT proliferation, whereas the addition of Toll-like receptor agonists causes high levels of activation and proliferation of the MAIT cell pool (Chen et al., 2017). It is possible that some pathogens provide higher amounts of MAIT-activating ligands or an inflammatory/cytokine context allowing larger cell expansion than other pathogens, as shown by the tremendous MAIT expansion in mice during *Francisella tularensis* infection (Meierovics et al., 2013). Several lines of evidence indicate that MAIT cells can adapt their proliferative and effector responses depending on the microbial and inflammatory signals present (López-Sagaseta et al., 2013; Gold et al., 2014; Slichter et al., 2016; Dias et al., 2017).

Our repertoire analysis of Vα7.2$^+$ CD161^{high} cord blood and adult subsets indicates that the fine specificity of the TCR conferred by the β chain must be important for 5-OP-RU recognition and expansion of Vα7.2$^+$ CD161^{high} T cells expressing the canonical MAIT TCR α chain. These results are consistent with structural data (Eckle et al., 2014). Only the few MR1:5-OP-RU reactive Vα7.2$^+$ CD161^{high} T cells that display a TRAV and TRBV repertoire very similar to adult MAIT cells expand in periphery to form the adult MAIT pool, diluting both the Vα7.2$^-$ CD161^{hi} and Vα7.2$^+$ CD161^{hi} MR1:5-OP-RU tetramer^{neg} T cells. Collectively, these results suggest that expansion of these few clones already present at birth is driven by repeated interactions with riboflavin-expressing pathogens encountered during the first years of life. Notably, MAIT cell levels exhibit very large interindividual variability (over one log range) in child and adult blood. It is tempting to speculate that microbial infection history contributes to the variable extent of MAIT cell expansion. Only a careful longitudinal analysis of MAIT levels in several populations of various ages in various environments will answer this question.

Although accurate identification of MAIT cells in tissues is limited in the absence of tetramer staining, Vα7.2$^+$ CD161^{high} cells have been found in fetal tissues (Leeansyah et al., 2014), and we detected them in the intestine of 1-mo-old babies. Of note, these cells are tissue-resident memory cells, unable to recirculate, as indicated by the entirely naive phenotype of circulating Vα7.2$^+$ CD161^{high} T cells at birth. Even in the absence of live microbes in the placenta, maternal gestational microbes might be a source of microbial-derived metabolites reaching fetal tissues, as recently demonstrated in a model of transient microbial colonization in pregnant mice (Gomez de Agüero et al., 2016). However, in contrast with their gradual expansion in peripheral blood after birth or cord blood transplantation, we found that Vα7.2$^+$ CD161^{high} cells did not accumulate much in intestinal tissues during childhood. The lack of any detectable Vα7.2$^+$ CD161^{high} cells in the intestine of HSCT recipients, in particular during the course of aGVHD, is quite surprising. Mucosal disruption, microbial translocation, and inflammation contribute to aGVHD pathogenesis and should allow at least a few graft-derived Vα7.2$^+$ CD161^{high} cells to rapidly home to mucosal sites. MAIT cells are highly sensitive to apoptotic stimuli (Gérart et al., 2013). One hypothesis is that microbial translocation triggers activation-induced apoptosis of newly generated MAIT cells within mucosal tissues or that post-transplant CS therapy exacerbates apoptotic sensitivity and prevents MAIT survival in tissues.

In addition to providing a more complete view of the physiological MAIT cell development, our results have important implications for appreciating the impact of MAIT cell loss in other situations. Thus, in line with our observation after cord blood transplantation, MAIT cells remained undetectable up to 2 yr after autologous HSCT in patients with multiple sclerosis (Abrahamsson et al., 2013). MAIT loss was correlated with good clinical response, supporting MAIT involvement in the disease pathology. Whether the benefit is still maintained at a time MAIT cells recover, i.e., 5–6 yr after transplantation, will deserve investigation. Our data may also explain the lack of circulating MAIT recovery in otherwise successfully treated HIV-infected patients (Cosgrove et al., 2013; Leeansyah et al., 2013). Rather than evoking an irreversible MAIT loss in a context of HIV infection, it is more likely that complete MAIT recovery requires a minimum of 5–6 yr after initiation of antiretroviral treatment, as indicated by our preliminary results on long-term treated HIV patients (M. Lambert and S. Caillat-Zucman, personal data).

Finally, our results indicate that the early expansion of MAIT cells after birth dilutes Vα7.2$^+$ CD161^{high} cells not reactive to 5-OP-RU presented by MR1. Part of these MR1:5-OP-RU tetramer^{neg} express the canonical MAIT TCR α chain and are thus likely selected on MR1 in the thymus. Because a formal demonstration of their MR1 restriction is not feasible in humans, single-cell TCR sequencing followed by TCR reexpression would be necessary to formally characterize the MR1:5-OP-RU tetramer^{neg} cells that express

the canonical TCR α chain. Whether these cells recognize empty MR1 or other MR1 ligand present during fetal life and around birth remains unknown. Nonstimulatory/inhibitory ligands, such as 6F-P and other pterin-based small drug-derived molecules, lead to high levels of MR1 surface expression and can inhibit MAIT cell activation by 5-OP-RU (Keller et al., 2017b). Such MR1 ligands might outcompete microbial ligands until those become quantitatively or qualitatively predominant after birth.

In conclusion, our in-depth analysis of the kinetics of MAIT cell development and its correlation with microbial or nonmicrobial environmental exposures highlights important defects in the newborn, as demonstrated for many other cellular and molecular components of innate immune responses (Kollmann et al., 2017). Whether this may contribute to the increased susceptibility of preterm neonates to severe microbial infections remains an open issue because selective MAIT cell deficiency has not been reported so far in humans. It is tempting to propose that neonatal and even prenatal (i.e., maternal) manipulation of MAIT cell numbers or functions by targeted interventions, such as exposure to probiotics or regulation of metabolic pathways, might optimize newborn defense toward severe microbial infections. The recent success of a synbiotic trial associating *Lactobacillus plantarum* to fructooligosaccharides to prevent sepsis in rural Indian newborns paves the way for such investigation (Panigrahi et al., 2017).

MATERIALS AND METHODS

Subjects

The first neonate cohort consisted of 153 consecutive newborns admitted at birth in the neonatology department and divided into four groups according to gestational age (GA): group 1, GA 24–27 wk ± 6 d (n = 28); group 2, GA 28–31 wk ± 6 d (n = 48); group 3, GA 32–36 wk ± 6 d (n = 41); group 4, term (>37 wk), hospitalized for jaundice, respiratory distress, or suspicion of early-onset infection (n = 36). Leftovers of systematic blood count tests performed during usual monitoring of the patients were obtained at birth (day 0, all groups), day 3 (all groups), day 30 (groups 1 and 2, and group 3 if the infant was still hospitalized), and day 60 (group 1, and group 2 if the infant was still hospitalized).

To confirm and extend the finding obtained from this first cohort, we included neonates from a second, independent cohort of 132 consecutive newborns similarly divided into four groups (group 1, n = 28; group 2, n = 32; group 3, n = 45; group 4, n = 27).

Mothers of newborns were sampled on the day of delivery. Whenever possible, pregnant women between 24 and 34 wk of gestation at risk of imminent preterm delivery were administered betamethasone (two 12-mg intramuscular doses 24 h apart) as the standard of childbirth care to improve newborn outcomes.

The cord blood transplant recipient group consisted of 17 consecutive children undergoing HSCT from UCB donors for a hematological malignancy in the hematology department between January 2013 and January 2015. Mean age at time of transplantation was 6.5 yr (range, 1.5–13 yr). Myeloablative conditioning regimen was provided either with VP16 associated to total body irradiation or with cyclophosphamide and busulfan. Primary prophylaxis of GVHD consisted of a calcineurin inhibitor and methylprednisolone (1 mg/kg/d 3 d before to 4 d after graft infusion, then 1.5 mg/kg/day until engraftment and subsequent tapering through day 45 in the absence of aGVHD or 2 mg/kg/day for 7 d and subsequent tapering through months in case of GVHD). Blood samples were obtained for assessment of immunological recovery at 1, 3, 6, and 12 mo after HSCT as the standard of care. To evaluate long-term recovery of MAIT cells, we analyzed blood samples taken 1–6 yr after HSCT in 20 additional UCB recipients at the time of a routine hospital visit.

Control peripheral blood samples were obtained from a first cohort of 79 healthy children aged 10 mo to 17 yr and a second cohort of 83 healthy infants aged 1 d to 12 mo (all sampled at the time of preoperative assessment or potential sibling donors of HSCT recipients) and 50 healthy adult blood donors (18–50 yr of age). Cord blood samples from full-term healthy neonates were obtained from the Department of Cellular Therapy (J. Larghero, Saint-Louis Hospital, Paris, France).

Cells and cell lines

Peripheral blood and cord blood mononuclear cells were isolated by Percoll density gradient centrifugation (Eurobio) and used immediately. Where indicated, CD8 T cells were enriched by using magnetic bead negative selection (Easy Sep Human CD8 isolation kit; Stemcell) per the manufacturer's instructions.

The THP1 cell line was cultured at 37°C in RPMI 1640 medium (Gibco) supplemented with 10% FCS and 1% penicillin and streptomycin.

Flow cytometry

MAIT cells were analyzed in parallel with other innate-like (Vα24$^+$ NKT cells and γδ T cells) and conventional αβ T lymphocytes on 100-µl residual whole blood within 24 h after collection. Multiparametric 10-color flow cytometry analyses were performed by using combinations of the following antibodies for 15 min at 4°C: anti-CD45 Krome Orange, anti-CD3 ECD, anti-CD8β PE or ECD, anti-TCR γδ PE Cy5.5, anti-TCR Vα24 PE Cy7 (all from Beckman Coulter); anti-TCR Vα7.2 FITC or APC (clone 3C10), anti-CD69 PeCy7, anti-CD25 BV421, anti-CD161 PerCP Cy5.5 or BV421, anti-CD4 AF700 (Biolegend); anti-CD161 APC, anti-CD3 APC Vio770 (Miltenyi); anti-CD4 APC AF750 (Invitrogen); anti-CD3 PerCP, anti-CD45RO FITC or APC AF700, anti-IL-12Rβ1 PE, anti-IL-12Rβ2 PE, anti-CD127 (IL-7R) BV421 (BD Biosciences); anti-IL-18Rα AF488 and anti-IL-23R PE (R&D); Zombie Aqua Live/Dead (BioLegend). For intracellular staining, cells were first stained with antibodies against surface antigens, then fixed/permeabilized, washed, and incubated with anti-Ki67

PE, anti-IFNγ FITC, anti-GrB PE, or anti-PLZF PE (BD Biosciences) at 4°C for 20 min. Data were acquired on a Navios flow cytometer (Beckman Coulter) collecting a total of at least 100,000 events in a live gate. Gates were defined through isotype and fluorescence-minus-one stains. The gating strategy was CD45 versus side scatter, and MAIT cells were defined as $CD3^+$ $CD4^-$ $TCR\gamma\delta^-$ $CD161^{high}$ $V\alpha7.2^+$ T cells. Frequencies were expressed as a percentage of $CD3^+$ lymphocytes. Absolute numbers (per microliter) were calculated from the absolute lymphocyte count determined on the same sample with a hematology automated analyzer. Where indicated, staining with the APC-conjugated MR1 :5-OP-RU or MR1:6-FP tetramer (dilution 1:600, NIH tetramer core facility) was performed for 45 min at room temperature before surface staining with other antibodies for 20 min at 4°C. Data were analyzed by using FlowJo software.

Functional assays

For proliferation assays, freshly purified peripheral blood, and cord blood mononuclear cells were labeled with 1 μM CFSE (Invitrogen) and cultured in the presence of 20 U/ml IL-2 with or without mitogen (5 μg/ml PHA) for 6 d.

For ex vivo stimulation assays, THP-1 cells were incubated with 1% paraformaldehyde-fixed *E. coli* (DH5α; S. Bonacorsi, Robert Debré Hospital, Paris, France) at 25 bacteria per cell for 24 h. Freshly isolated CD8 T cells were cultured overnight in the presence of THP-1/*E. coli*, or THP-1 alone as negative control, at a 1:1 THP1/CD8 T cell ratio. Brefeldin A was added for the last 3 h. Alternatively, cells were stimulated for 5 or 12 h with 50 ng/ml PMA plus 250 ng/ml ionomycin or with a combination of 10 ng/ml IL-12 and 100 ng/ml IL-18 (R&D).

Tissue analysis

Intestinal tissue leftovers from different anatomical locations were obtained from children undergoing various surgical procedures. Control samples were taken from uninvolved intestine segments after surgical resection for bowel perforation, volvulus, or stenosis ($n = 8$). In addition, tissues were obtained from children undergoing surgery for appendicitis ($n = 5$) or necrotizing enterocolitis ($n = 3$).

For ex vivo analysis of infiltrating lymphocytes, intestinal tissues were cut into small pieces and washed in PBS. The mucosa was separated from the serosa with scissors, cut into 1–5-mm strips, and incubated for 15 min at 22°C in serum-free RPMI medium with 200 μg/ml type II DNase I (Sigma-Aldrich). The remaining mucosa strips were gently crushed and filtered through 40-μm cell strainers to isolate mucosal mononuclear cells. Cells were immediately stained and analyzed by flow cytometry.

For immunohistochemical analysis, 5-μm-thick formalin-fixed, paraffin-embedded tissue sections were prepared from surgically resected intestinal tissues ($n = 8$ patients) and intestinal biopsies taken for diagnostic purposes in HSCT recipients (aGVHD, $n = 5$ vs. viral infection, $n = 4$). In brief, serial sections were incubated for 15 min at room temperature with anti-CD3, anti-CD8 (BD BioSciences), or anti-Vα7.2 (Biolegend) antibodies, detected by polymeric alkaline phosphatase (AP)– or horseradish peroxidase (HRP)–linker antibody conjugate (Bond Polymer Refine Detection, Novocastra; Leica Biosystems). Slides were counterstained with hematoxylin and observed with Leica DM4000 B Led microscope. Images were processed with a DFC 310 FX camera (Leica Microsystems).

qPCR analysis for MAIT α chain expression

RNA was extracted from FACS-sorted CD3+ CD4- $V\alpha7.2^+$ $CD161^{high}$ and $CD161^-$ populations (2,500–8,000 cells) in RLT using a single cell RNA purification kit (Norgen) with an on-column DNase step (Qiagen), according to the manufacturer's guidelines. RNA integrity was checked on a bioanalyzer by using a pico chip (Agilent Technologies). Reverse transcription was performed with the Superscript II (Invitrogen) enzyme by using 12.5 μg/ml random primers and oligodT. qPCR was realized on a Light Cycler 480 (Roche) by using the Light Cycler 480 probe master mix (Roche) and the following primers (Eurogentec): Vα7.2 for (5′-TCC TTAGTCGGTCTAAAGGGTACAG-3′) and Jα33 rev (5′-CCCAGCGCCCCAGATTAA-3′) or Cα rev1 (5′-GGC AGACAGACTTGTCACTGGAT-3′) for TRAV amplification, Cα for (5′-ACCCTGACCCTGCCGTGT-3′), and Cα rev2 (5′-GGCTGGGGAAGAAGGTGTCTT-3′) for TRAC amplification. MGB probes (Thermo Fisher Scientific) were added for detection: Vα7.2 (5′-TGAAAGACTCTGCCT CTTACCTCTGTGC-3′) and Cα (5′-GCATGTGCAAAC GCCTTCAACAACA-3′). Relative expression was calculated by using the 2-ddCt method, and the median of adult Vα7.2-Jα33 expression was set to 100% expression.

TRAV1-2 and TCRβ repertoire analysis by multiplex PCR and high-throughput sequencing

RNA extraction and RT were performed on FACS-sorted populations (2,500–8,000 cells for bulk $V\alpha7.2^+$ populations, 50 and 1,000 cells for $V\alpha7.2^+$ $CD161^{high}$ MR1:5-OP-RU^+ and MR1:5-OP-RU^- populations, respectively) by using the same protocol as for the qPCR. Two semi-nested PCR were realized by using only the TRAV1 primer for the α chain and a pool of β chain primers, as described in (Han et al., 2014). Fluidigm barcodes were added by a third PCR on purified PCR products (Agencourt AMPure XP beads; Beckman Coulter), and sequencing was performed by the Institut Curie NGS platform on a MiSeq apparatus (Illumina-V2-2*250 base-paired end reads). Only predicted productive TCR rearrangements with more than one read were kept for downstream analysis.

TCRβ repertoire analysis by RACE technique

TCRβ repertoires were obtained using a modified 5′RACE technique as described (Vera et al., 2013). The libraries were sequenced by using either an Ion PGM (Ion 318 Chip vx

400 base reads Life Technologies) or a MiSeq (Illumina–v3 kit–2 × 300 base paired end reads) apparatus on the ICGEX platform (Institut Curie) as described in (Cui et al., 2015). Each dataset was demultiplexed and trimmed for base quality (>25) and read length (>250 bp). Paired reads were merged by using flash v1.2.10 program (-m30-M135-t10-×0.1; Magoč and Salzberg, 2011). Resulting fasta files were then uploaded onto IMGT/high V-Quest webserver (Li et al., 2013; allele*01 only), and the "Junction" file was parsed by using an in-house R script to extract information regarding the V-J combination and the CDR3 nucleotidic composition. Only predicted productive TCR rearrangements were kept for downstream analysis. β-repertoire sequencing data were analyzed by using R (R Development Core Team, 2012) and vegan packages. To normalize for uneven numbers of reads, each dataset was subsampled 100 times at 5,000 reads depth. Then an average rarefaction matrix was computed from the 100 subsampled tables. Rarefaction plots were computed by using the average rarefied matrix.

Statistical analysis

Differences between groups were analyzed by using non-parametric tests for paired (Wilcoxon) and unpaired (Mann–Whitney or Kruskall–Wallis) groups or one-way ANOVA with posttest for linear trend. Error bars represent SEM unless otherwise specified. Correlations were assessed by using the Spearman rank correlation. Linear regression analysis was used to test associations between the log-transformed cell levels and clinical variables. Two-sided p-values <0.05 were considered significant. No statistical method was used to predetermine sample size. Analyses were performed by using Prism software v.6 (GraphPad).

Study approval

The study was performed with the approval of the Robert Debré Hospital Ethics Committee (HREC 2013/49) and the CPP Ile de France IV (2015/03NICB), in agreement with the principles of the Declaration of Helsinki and French legislation. All subjects (or their parents) provided written, informed consent. The study was registered in a public trial registry: ClinicalTrials.gov number NCT02403089.

Online supplemental material

Fig. S1 shows absolute numbers of $V\alpha7.2^+$ $CD161^{high}$ T cells and related T cell subsets in the first neonate cohort, and their frequencies in the two combined cohorts. Fig. S2 shows the proportion of MR1:5-OP-RU $tetramer^{pos}$ and $tetramer^{neg}$ $V\alpha7.2^+$ $CD161^{high}$ T cells during the first year of life. Fig. S3 shows the TCRβ repertoire analysis (rarefaction curves) of MAIT cells and related T cell subsets in 4 cord blood and 13 adult blood samples. Fig. S4 shows the TRBV and TRBJ fragment usage of $V\alpha7.2^+$ $CD161^{high}$ T cells in 4 cord blood and 14 adult blood samples. Fig. S5 shows the comparison of the TRBV and TRBJ fragment usage in MAIT cells and related T cell subsets in 4 cord blood samples.

ACKNOWLEDGMENTS

We thank all the patients and their physicians and the nurse and technician staff from Hôpital Robert Debré who helped with this study. We also thank Adam Woolfe for preliminary analysis of the sequencing data following multiplex PCR.

This work was supported by grants from Agence Nationale de la Recherche (ANR) and Direction Générale de l'Offre de Soins (DGOS; PRTS 14-CE15-0005, acronym NEOMAIT), Institut National du Cancer (INCa; 2012-059), Agence de Biomédecine, Cent pour Sang la vie, IRGHET, and Fondation pour la Recherche Médicale (FRM; ING20150532367). High-throughput sequencing was performed by the ICGex NGS platform of the Institut Curie supported by Agence Nationale de la Recherche grants (ANR-10-EQPX-03, Equipex; and ANR-10-INBS-09-08, France Génomique Consortium) from the "Investissements d'Avenir" program, the Canceropole Ile-de-France, and the SiRIC-Curie program (grant INCa-DGOS-4654).

The authors declare no competing financial interests.

Author contributions: G. Ben Youssef, M. Tourret, M. Salou, L. Ghazarian, S. Mondot, Y. Mburu, M. Lambert, S. Azarnoush, J.-S. Diana, and A.-L. Virlouvet designed research studies, conducted experiments, analyzed data, and/or provided patient samples. V. Houdouin and M. Peuchmaur analyzed data. J.-H. Dalle, O. Lantz, and V. Biran designed research studies, analyzed data, and wrote the manuscript. S. Caillat-Zucman designed research studies, supervised the study, analyzed data, and wrote the manuscript with the help of other coauthors.

Submitted: 21 September 2017

Revised: 27 October 2017

Accepted: 6 December 2017

REFERENCES

Abrahamsson, S.V., D.F. Angelini, A.N. Dubinsky, E. Morel, U. Oh, J.L. Jones, D. Carassiti, R. Reynolds, M. Salvetti, P.A. Calabresi, et al. 2013. Non-myeloablative autologous haematopoietic stem cell transplantation expands regulatory cells and depletes IL-17 producing mucosal-associated invariant T cells in multiple sclerosis. *Brain*. 136:2888–2903. https://doi.org/10.1093/brain/awt182

Adkins, B., C. Leclerc, and S. Marshall-Clarke. 2004. Neonatal adaptive immunity comes of age. *Nat. Rev. Immunol.* 4:553–564. https://doi.org/10.1038/nri1394

Billerbeck, E., Y.H. Kang, L. Walker, H. Lockstone, S. Grafmueller, V. Fleming, J. Flint, C.B. Willberg, B. Bengsch, B. Seigel, et al. 2010. Analysis of CD161 expression on human CD8+ T cells defines a distinct functional subset with tissue-homing properties. *Proc. Natl. Acad. Sci. USA*. 107:3006–3011. https://doi.org/10.1073/pnas.0914839107

Booth, J.S., R. Salerno-Goncalves, T.G. Blanchard, S.A. Patil, H.A. Kader, A.M. Safta, L.M. Morningstar, S.J. Czinn, B.D. Greenwald, and M.B. Sztein. 2015. Mucosal-associated invariant T cells in the human gastric mucosa and blood: Role in helicobacter pylori infection. *Front. Immunol.* 6:466. https://doi.org/10.3389/fimmu.2015.00466

Chen, Z., H. Wang, C. D'Souza, S. Sun, L. Kostenko, S.B. Eckle, B.S. Meehan, D.C. Jackson, R.A. Strugnell, H. Cao, et al. 2017. Mucosal-associated invariant T-cell activation and accumulation after in vivo infection depends on microbial riboflavin synthesis and co-stimulatory signals. *Mucosal Immunol.* 10:58–68. https://doi.org/10.1038/mi.2016.39

Corbett, A.J., S.B. Eckle, R.W. Birkinshaw, L. Liu, O. Patel, J. Mahony, Z. Chen, R. Reantragoon, B. Meehan, H. Cao, et al. 2014. T-cell activation by transitory neo-antigens derived from distinct microbial pathways. *Nature*. 509:361–365. https://doi.org/10.1038/nature13160

Cosgrove, C., J.E. Ussher, A. Rauch, K. Gärtner, A. Kurioka, M.H. Hühn, K. Adelmann, Y.H. Kang, J.R. Fergusson, P. Simmonds, et al. 2013. Early and nonreversible decrease of CD161++ /MAIT cells in HIV infection. *Blood*. 121:951–961. https://doi.org/10.1182/blood-2012-06-436436

Cui, Y., K. Franciszkiewicz, Y.K. Mburu, S. Mondot, L. Le Bourhis, V. Premel, E. Martin, A. Kachaner, L. Duban, M.A. Ingersoll, et al. 2015. Mucosal-associated invariant T cell-rich congenic mouse strain allows functional

evaluation. *J. Clin. Invest.* 125:4171–4185. https://doi.org/10.1172/JCI82424

Dias, J., E. Leeansyah, and J.K. Sandberg. 2017. Multiple layers of heterogeneity and subset diversity in human MAIT cell responses to distinct microorganisms and to innate cytokines. *Proc. Natl. Acad. Sci. USA.* 114:E5434–E5443. https://doi.org/10.1073/pnas.1705759114

Dominguez-Bello, M.G., E.K. Costello, M. Contreras, M. Magris, G. Hidalgo, N. Fierer, and R. Knight. 2010. Delivery mode shapes the acquisition and structure of the initial microbiota across multiple body habitats in newborns. *Proc. Natl. Acad. Sci. USA.* 107:11971–11975. https://doi.org/10.1073/pnas.1002601107

Dusseaux, M., E. Martin, N. Serriari, I. Péguillet, V. Premel, D. Louis, M. Milder, L. Le Bourhis, C. Soudais, E. Treiner, and O. Lantz. 2011. Human MAIT cells are xenobiotic-resistant, tissue-targeted, CD161hi IL-17-secreting T cells. *Blood.* 117:1250–1259. https://doi.org/10.1182/blood-2010-08-303339

Eckle, S.B., R.W. Birkinshaw, L. Kostenko, A.J. Corbett, H.E. McWilliam, R. Reantragoon, Z. Chen, N.A. Gherardin, T. Beddoe, L. Liu, et al. 2014. A molecular basis underpinning the T cell receptor heterogeneity of mucosal-associated invariant T cells. *J. Exp. Med.* 211:1585–1600. https://doi.org/10.1084/jem.20140484

Fergusson, J.R., M.H. Hühn, L. Swadling, L.J. Walker, A. Kurioka, A. Llibre, A. Bertoletti, G. Holländer, E.W. Newell, M.M. Davis, et al. 2016. CD161(int)CD8+ T cells: a novel population of highly functional, memory CD8+ T cells enriched within the gut. *Mucosal Immunol.* 9:401–413. https://doi.org/10.1038/mi.2015.69

Georgel, P., M. Radosavljevic, C. Macquin, and S. Bahram. 2011. The non-conventional MHC class I MR1 molecule controls infection by Klebsiella pneumoniae in mice. *Mol. Immunol.* 48:769–775. https://doi.org/10.1016/j.molimm.2010.12.002

Gérart, S., S. Sibéril, E. Martin, C. Lenoir, C. Aguilar, C. Picard, O. Lantz, A. Fischer, and S. Latour. 2013. Human iNKT and MAIT cells exhibit a PLZF-dependent proapoptotic propensity that is counterbalanced by XIAP. *Blood.* 121:614–623. https://doi.org/10.1182/blood-2012-09-456095

Gold, M.C., S. Cerri, S. Smyk-Pearson, M.E. Cansler, T.M. Vogt, J. Delepine, E. Winata, G.M. Swarbrick, W.J. Chua, Y.Y. Yu, et al. 2010. Human mucosal associated invariant T cells detect bacterially infected cells. *PLoS Biol.* 8:e1000407. https://doi.org/10.1371/journal.pbio.1000407

Gold, M.C., J.E. McLaren, J.A. Reistetter, S. Smyk-Pearson, K. Ladell, G.M. Swarbrick, Y.Y. Yu, T.H. Hansen, O. Lund, M. Nielsen, et al. 2014. MR1-restricted MAIT cells display ligand discrimination and pathogen selectivity through distinct T cell receptor usage. *J. Exp. Med.* 211:1601–1610. https://doi.org/10.1084/jem.20140507

Gomez de Agüero, M., S.C. Ganal-Vonarburg, T. Fuhrer, S. Rupp, Y. Uchimura, H. Li, A. Steinert, M. Heikenwalder, S. Hapfelmeier, U. Sauer, et al. 2016. The maternal microbiota drives early postnatal innate immune development. *Science.* 351:1296–1302. https://doi.org/10.1126/science.aad2571

Grimaldi, D., L. Le Bourhis, B. Sauneuf, A. Dechartres, C. Rousseau, F. Ouaaz, M. Milder, D. Louis, J.D. Chiche, J.P. Mira, et al. 2014. Specific MAIT cell behaviour among innate-like T lymphocytes in critically ill patients with severe infections. *Intensive Care Med.* 40:192–201. https://doi.org/10.1007/s00134-013-3163-x

Han, A., J. Glanville, L. Hansmann, and M.M. Davis. 2014. Linking T-cell receptor sequence to functional phenotype at the single-cell level. *Nat. Biotechnol.* 32:684–692. https://doi.org/10.1038/nbt.2938

Hingorani, R., I.H. Choi, P. Akolkar, B. Gulwani-Akolkar, R. Pergolizzi, J. Silver, and P.K. Gregersen. 1993. Clonal predominance of T cell receptors within the CD8+ CD45RO+ subset in normal human subjects. *J. Immunol.* 151:5762–5769.

Hinks, T.S., X. Zhou, K.J. Staples, B.D. Dimitrov, A. Manta, T. Petrossian, P.Y. Lum, C.G. Smith, J.A. Ward, P.H. Howarth, et al. 2015. Innate and adaptive T cells in asthmatic patients: Relationship to severity and disease mechanisms. *J. Allergy Clin. Immunol.* 136:323–333. https://doi.org/10.1016/j.jaci.2015.01.014

Hinks, T.S., J.C. Wallington, A.P. Williams, R. Djukanović, K.J. Staples, and T.M. Wilkinson. 2016. Steroid-induced deficiency of mucosal-associated invariant T cells in the chronic obstructive pulmonary disease lung. Implications for nontypeable Haemophilus influenzae infection. *Am. J. Respir. Crit. Care Med.* 194:1208–1218. https://doi.org/10.1164/rccm.201601-0002OC

Keller, A.N., A.J. Corbett, J.M. Wubben, J. McCluskey, and J. Rossjohn. 2017a. MAIT cells and MR1-antigen recognition. *Curr. Opin. Immunol.* 46:66–74. https://doi.org/10.1016/j.coi.2017.04.002

Keller, A.N., S.B. Eckle, W. Xu, L. Liu, V.A. Hughes, J.Y. Mak, B.S. Meehan, T. Pediongco, R.W. Birkinshaw, Z. Chen, et al. 2017b. Drugs and drug-like molecules can modulate the function of mucosal-associated invariant T cells. *Nat. Immunol.* 18:402–411. https://doi.org/10.1038/ni.3679

Kjer-Nielsen, L., O. Patel, A.J. Corbett, J. Le Nours, B. Meehan, L. Liu, M. Bhati, Z. Chen, L. Kostenko, R. Reantragoon, et al. 2012. MR1 presents microbial vitamin B metabolites to MAIT cells. *Nature.* 491:717–723. https://doi.org/10.1038/nature11605

Koay, H.F., N.A. Gherardin, A. Enders, L. Loh, L.K. Mackay, C.F. Almeida, B.E. Russ, C.A. Nold-Petry, M.F. Nold, S. Bedoui, et al. 2016. A three-stage intrathymic development pathway for the mucosal-associated invariant T cell lineage. *Nat. Immunol.* 17:1300–1311. https://doi.org/10.1038/ni.3565

Kollmann, T.R., B. Kampmann, S.K. Mazmanian, A. Marchant, and O. Levy. 2017. Protecting the newborn and young infant from infectious diseases: Lessons from immune ontogeny. *Immunity.* 46:350–363. https://doi.org/10.1016/j.immuni.2017.03.009

Kovalovsky, D., O.U. Uche, S. Eladad, R.M. Hobbs, W. Yi, E. Alonzo, K. Chua, M. Eidson, H.J. Kim, J.S. Im, et al. 2008. The BTB-zinc finger transcriptional regulator PLZF controls the development of invariant natural killer T cell effector functions. *Nat. Immunol.* 9:1055–1064. https://doi.org/10.1038/ni.1641

Kurioka, A., J.E. Ussher, C. Cosgrove, C. Clough, J.R. Fergusson, K. Smith, Y.H. Kang, L.J. Walker, T.H. Hansen, C.B. Willberg, and P. Klenerman. 2015. MAIT cells are licensed through granzyme exchange to kill bacterially sensitized targets. *Mucosal Immunol.* 8:429–440. https://doi.org/10.1038/mi.2014.81

Le Bourhis, L., E. Martin, I. Péguillet, A. Guihot, N. Froux, M. Coré, E. Lévy, M. Dusseaux, V. Meyssonnier, V. Premel, et al. 2010. Antimicrobial activity of mucosal-associated invariant T cells. *Nat. Immunol.* 11:701–708. https://doi.org/10.1038/ni.1890

Le Bourhis, L., M. Dusseaux, A. Bohineust, S. Bessoles, E. Martin, V. Premel, M. Coré, D. Sleurs, N.E. Serriari, E. Treiner, et al. 2013. MAIT cells detect and efficiently lyse bacterially-infected epithelial cells. *PLoS Pathog.* 9:e1003681. https://doi.org/10.1371/journal.ppat.1003681

Leeansyah, E., A. Ganesh, M.F. Quigley, A. Sönnerborg, J. Andersson, P.W. Hunt, M. Somsouk, S.G. Deeks, J.N. Martin, M. Moll, et al. 2013. Activation, exhaustion, and persistent decline of the antimicrobial MR1-restricted MAIT-cell population in chronic HIV-1 infection. *Blood.* 121:1124–1135. https://doi.org/10.1182/blood-2012-07-445429

Leeansyah, E., L. Loh, D.F. Nixon, and J.K. Sandberg. 2014. Acquisition of innate-like microbial reactivity in mucosal tissues during human fetal MAIT-cell development. *Nat. Commun.* 5:3143. https://doi.org/10.1038/ncomms4143

Legoux, F., M. Salou, and O. Lantz. 2017. Unconventional or preset αβ T cells: Evolutionarily conserved tissue-resident T cells recognizing nonpeptidic ligands. *Annu. Rev. Cell Dev. Biol.* 33:511–535. https://doi.org/10.1146/annurev-cellbio-100616-060725

Lepore, M., A. Kalinichenko, A. Colone, B. Paleja, A. Singhal, A. Tschumi, B. Lee, M. Poidinger, F. Zolezzi, L. Quagliata, et al. 2014. Parallel T-cell cloning and deep sequencing of human MAIT cells reveal stable

oligoclonal TCRβ repertoire. *Nat. Commun.* 5:3866. https://doi.org/10.1038/ncomms4866

Leung, D.T., T.R. Bhuiyan, N.S. Nishat, M.R. Hoq, A. Aktar, M.A. Rahman, T. Uddin, A.I. Khan, F. Chowdhury, R.C. Charles, et al. 2014. Circulating mucosal associated invariant T cells are activated in Vibrio cholerae O1 infection and associated with lipopolysaccharide antibody responses. *PLoS Negl. Trop. Dis.* 8:e3076. https://doi.org/10.1371/journal.pntd.0003076

Levy, O. 2007. Innate immunity of the newborn: basic mechanisms and clinical correlates. *Nat. Rev. Immunol.* 7:379–390. https://doi.org/10.1038/nri2075

Li, S., M.P. Lefranc, J.J. Miles, E. Alamyar, V. Giudicelli, P. Duroux, J.D. Freeman, V.D. Corbin, J.P. Scheerlinck, M.A. Frohman, et al. 2013. IMGT/HighV QUEST paradigm for T cell receptor IMGT clonotype diversity and next generation repertoire immunoprofiling. *Nat. Commun.* 4:2333. https://doi.org/10.1038/ncomms3333

Loh, L., Z. Wang, S. Sant, M. Koutsakos, S. Jegaskanda, A.J. Corbett, L. Liu, D.P. Fairlie, J. Crowe, J. Rossjohn, et al. 2016. Human mucosal-associated invariant T cells contribute to antiviral influenza immunity via IL-18-dependent activation. *Proc. Natl. Acad. Sci. USA.* 113:10133–10138. https://doi.org/10.1073/pnas.1610750113

López-Sagaseta, J., C.L. Dulberger, J.E. Crooks, C.D. Parks, A.M. Luoma, A. McFedries, I. Van Rhijn, A. Saghatelian, and E.J. Adams. 2013. The molecular basis for Mucosal-Associated Invariant T cell recognition of MR1 proteins. *Proc. Natl. Acad. Sci. USA.* 110:E1771–E1778. https://doi.org/10.1073/pnas.1222678110

Maggi, L., V. Santarlasci, M. Capone, A. Peired, F. Frosali, S.Q. Crome, V. Querci, M. Fambrini, F. Liotta, M.K. Levings, et al. 2010. CD161 is a marker of all human IL-17-producing T-cell subsets and is induced by RORC. *Eur. J. Immunol.* 40:2174–2181. https://doi.org/10.1002/eji.200940257

Magoč, T., and S.L. Salzberg. 2011. FLASH: Fast length adjustment of short reads to improve genome assemblies. *Bioinformatics.* 27:2957–2963. https://doi.org/10.1093/bioinformatics/btr507

Martin, E., E. Treiner, L. Duban, L. Guerri, H. Laude, C. Toly, V. Premel, A. Devys, I.C. Moura, F. Tilloy, et al. 2009. Stepwise development of MAIT cells in mouse and human. *PLoS Biol.* 7:e54. https://doi.org/10.1371/journal.pbio.1000054

Meierovics, A.I., and S.C. Cowley. 2016. MAIT cells promote inflammatory monocyte differentiation into dendritic cells during pulmonary intracellular infection. *J. Exp. Med.* 213:2793–2809. https://doi.org/10.1084/jem.20160637

Meierovics, A., W.J. Yankelevich, and S.C. Cowley. 2013. MAIT cells are critical for optimal mucosal immune responses during in vivo pulmonary bacterial infection. *Proc. Natl. Acad. Sci. USA.* 110:E3119–E3128. https://doi.org/10.1073/pnas.1302799110

Mondot, S., P. Boudinot, and O. Lantz. 2016. MAIT, MR1, microbes and riboflavin: A paradigm for the co-evolution of invariant TCRs and restricting MHCI-like molecules? *Immunogenetics.* 68:537–548. https://doi.org/10.1007/s00251-016-0927-9

Neu, J., and W.A. Walker. 2011. Necrotizing enterocolitis. *N. Engl. J. Med.* 364:255–264. https://doi.org/10.1056/NEJMra1005408

Panigrahi, P., S. Parida, N.C. Nanda, R. Satpathy, L. Pradhan, D.S. Chandel, L. Baccaglini, A. Mohapatra, S.S. Mohapatra, P.R. Misra, et al. 2017. A randomized synbiotic trial to prevent sepsis among infants in rural India. *Nature.* 548:407–412. https://doi.org/10.1038/nature23480

Rahimpour, A., H.F. Koay, A. Enders, R. Clanchy, S.B. Eckle, B. Meehan, Z. Chen, B. Whittle, L. Liu, D.P. Fairlie, et al. 2015. Identification of phenotypically and functionally heterogeneous mouse mucosal-associated invariant T cells using MR1 tetramers. *J. Exp. Med.* 212:1095–1108. https://doi.org/10.1084/jem.20142110

Reantragoon, R., A.J. Corbett, I.G. Sakala, N.A. Gherardin, J.B. Furness, Z. Chen, S.B. Eckle, A.P. Uldrich, R.W. Birkinshaw, O. Patel, et al. 2013. Antigen-loaded MR1 tetramers define T cell receptor heterogeneity in mucosal-associated invariant T cells. *J. Exp. Med.* 210:2305–2320. https://doi.org/10.1084/jem.20130958

Rubens, C.E., Y. Sadovsky, L. Muglia, M.G. Gravett, E. Lackritz, and C. Gravett. 2014. Prevention of preterm birth: harnessing science to address the global epidemic. *Sci. Transl. Med.* 6:262sr5. https://doi.org/10.1126/scitranslmed.3009871

Sathaliyawala, T., M. Kubota, N. Yudanin, D. Turner, P. Camp, J.J. Thome, K.L. Bickham, H. Lerner, M. Goldstein, M. Sykes, et al. 2013. Distribution and compartmentalization of human circulating and tissue-resident memory T cell subsets. *Immunity.* 38:187–197. https://doi.org/10.1016/j.immuni.2012.09.020

Savage, A.K., M.G. Constantinides, J. Han, D. Picard, E. Martin, B. Li, O. Lantz, and A. Bendelac. 2008. The transcription factor PLZF directs the effector program of the NKT cell lineage. *Immunity.* 29:391–403. https://doi.org/10.1016/j.immuni.2008.07.011

Serriari, N.E., M. Eoche, L. Lamotte, J. Lion, M. Fumery, P. Marcelo, D. Chatelain, A. Barre, E. Nguyen-Khac, O. Lantz, et al. 2014. Innate mucosal-associated invariant T (MAIT) cells are activated in inflammatory bowel diseases. *Clin. Exp. Immunol.* 176:266–274. https://doi.org/10.1111/cei.12277

Slichter, C.K., A. McDavid, H.W. Miller, G. Finak, B.J. Seymour, J.P. McNevin, G. Diaz, J.L. Czartoski, M.J. McElrath, R. Gottardo, and M. Prlic. 2016. Distinct activation thresholds of human conventional and innate-like memory T cells. *JCI Insight.* 1:e86292. https://doi.org/10.1172/jci.insight.86292

Smith, D.J., G.R. Hill, S.C. Bell, and D.W. Reid. 2014. Reduced mucosal associated invariant T-cells are associated with increased disease severity and Pseudomonas aeruginosa infection in cystic fibrosis. *PLoS One.* 9:e109891. https://doi.org/10.1371/journal.pone.0109891

Sundström, P., F. Ahlmanner, P. Akéus, M. Sundquist, S. Alsén, U. Yrlid, L. Börjesson, Å. Sjöling, B. Gustavsson, S.B. Wong, and M. Quiding-Järbrink. 2015. Human mucosa-associated invariant T cells accumulate in colon adenocarcinomas but produce reduced amounts of IFN-γ. *J. Immunol.* 195:3472–3481. https://doi.org/10.4049/jimmunol.1500258

Thome, J.J., N. Yudanin, Y. Ohmura, M. Kubota, B. Grinshpun, T. Sathaliyawala, T. Kato, H. Lerner, Y. Shen, and D.L. Farber. 2014. Spatial map of human T cell compartmentalization and maintenance over decades of life. *Cell.* 159:814–828. https://doi.org/10.1016/j.cell.2014.10.026

Thome, J.J., K.L. Bickham, Y. Ohmura, M. Kubota, N. Matsuoka, C. Gordon, T. Granot, A. Griesemer, H. Lerner, T. Kato, and D.L. Farber. 2016. Early-life compartmentalization of human T cell differentiation and regulatory function in mucosal and lymphoid tissues. *Nat. Med.* 22:72–77. https://doi.org/10.1038/nm.4008

Tilloy, F., E. Treiner, S.H. Park, C. Garcia, F. Lemonnier, H. de la Salle, A. Bendelac, M. Bonneville, and O. Lantz. 1999. An invariant T cell receptor alpha chain defines a novel TAP-independent major histocompatibility complex class Ib-restricted alpha/beta T cell subpopulation in mammals. *J. Exp. Med.* 189:1907–1921. https://doi.org/10.1084/jem.189.12.1907

Treiner, E., L. Duban, S. Bahram, M. Radosavljevic, V. Wanner, F. Tilloy, P. Affaticati, S. Gilfillan, and O. Lantz. 2003. Selection of evolutionarily conserved mucosal-associated invariant T cells by MR1. *Nature.* 422:164–169. https://doi.org/10.1038/nature01433

Turtle, C.J., J. Delrow, R.C. Joslyn, H.M. Swanson, R. Basom, L. Tabellini, C. Delaney, S. Heimfeld, J.A. Hansen, and S.R. Riddell. 2011. Innate signals overcome acquired TCR signaling pathway regulation and govern the fate of human CD161(hi) CD8α^+ semi-invariant T cells. *Blood.* 118:2752–2762. https://doi.org/10.1182/blood-2011-02-334698

Ussher, J.E., M. Bilton, E. Attwod, J. Shadwell, R. Richardson, C. de Lara, E. Mettke, A. Kurioka, T.H. Hansen, P. Klenerman, and C.B. Willberg. 2014. CD161++ CD8+ T cells, including the MAIT cell subset, are specifically activated by IL-12+IL-18 in a TCR-independent manner. *Eur. J. Immunol.* 44:195–203. https://doi.org/10.1002/eji.201343509

Van Rhijn, I., A. Kasmar, A. de Jong, S. Gras, M. Bhati, M.E. Doorenspleet, N. de Vries, D.I. Godfrey, J.D. Altman, W. de Jager, et al. 2013. A conserved human T cell population targets mycobacterial antigens presented by CD1b. *Nat. Immunol.* 14:706–713. https://doi.org/10.1038/ni.2630

van Wilgenburg, B., I. Scherwitzl, E.C. Hutchinson, T. Leng, A. Kurioka, C. Kulicke, C. de Lara, S. Cole, S. Vasanawathana, W. Limpitikul, et al. STOP-HCV consortium. 2016. MAIT cells are activated during human viral infections. *Nat. Commun.* 7:11653. https://doi.org/10.1038/ncomms11653

Vera, G., P. Rivera-Munoz, V. Abramowski, L. Malivert, A. Lim, C. Bole-Feysot, C. Martin, B. Florkin, S. Latour, P. Revy, and J.P. de Villartay. 2013. Cernunnos deficiency reduces thymocyte life span and alters the T cell repertoire in mice and humans. *Mol. Cell. Biol.* 33:701–711. https://doi.org/10.1128/MCB.01057-12

Walker, L.J., Y.H. Kang, M.O. Smith, H. Tharmalingham, N. Ramamurthy, V.M. Fleming, N. Sahgal, A. Leslie, Y. Oo, A. Geremia, et al. 2012. Human MAIT and CD8αα cells develop from a pool of type-17 precommitted CD8+ T cells. *Blood.* 119:422–433. https://doi.org/10.1182/blood-2011-05-353789